# Contribution of soil elemental contents and Cu and Sr isotope ratios to the understanding of pedogenetic processes and mechanisms involved in the soil-to-grape transfer (Soave vineyard, Italy)

Simon Blotevogel, Eva Schreck, Stéphane Audry, Giuseppe Saldi, Jérôme Viers, Pierre Courjault-Radé, José Darrozes, Laurent Orgogozo, Priscia Oliva

# Contribution of soil elemental contents and Cu and Sr isotope ratios to the understanding of pedogenetic processes and mechanisms involved in the soil-to-grape transfer (Soave vineyard, Italy)

Simon Blotevogel[1,a], Eva Schreck[1,*], Stéphane Audry[1], Giuseppe D. Saldi[1], Jérôme Viers[1], Pierre Courjault-Radé[1], José Darrozes[1], Laurent Orgogozo[1], Priscia Oliva[1]

[1] Géosciences Environnement Toulouse (GET), Observatoire Midi Pyrénées, Université de Toulouse, CNRS, IRD, 14 avenue E. Belin, 31400 Toulouse, France.

[a] Present address: Laboratoire Matériaux et Durabilité des Constructions (LMDC), Université de Toulouse (INSAT/UPS), Génie Civil, 135 Avenue de Rangueil, 31077 Toulouse Cedex 04, France

** corresponding author:* eva.schreck@get.omp.eu ; + 33 5 61 33 26 76

**Abstract**

The effect of soil on wine composition and flavor is controversially discussed in viticulture. Mineral nutrition of the grapevine is one possibility for an influence of soil chemistry on winemaking. However, effects of soil chemistry are difficult to isolate from other physical and biological factors.

Here two winegrowing plots in the Soave region (Italy) were investigated, lying side by side on contrasted soil types. Factors that influenced soil formation and characterize soil chemistry and mineralogy were determined. The influence of soil type on the elemental composition (Mg, Al, P, S, K, Ca, Mn, Fe, Cu, Zn, Sr, Mo and Ba) of leaves and grapes was studied. Carbon isotope ratios were measured to evaluate water stress. Radiogenic Sr and stable Cu isotope ratios were studied to identify the influence of different bedrocks and better understand the mechanisms involved in the soil-to-grape continuum.

Even though the morphology of soils is different, chemical characteristics are similar in both vineyard plots. Nevertheless, Sr isotope ratios of horizons of both soils show influence of different bedrocks on their genesis. The composition of grapevine plants is similar between both plots even though there is a tendency for higher elemental contents on more calcareous soil. Finally, isotope ratios show that different mechanisms control Cu and Sr in plant: Cu seems to be controlled by regulation mechanisms of the plants whereas Sr is absorbed in ratios similar to the soil, reflecting the different geological origins.

**Keywords:** vineyard soil; mineral nutrition; soil formation; element transfers; Sr and Cu isotopes

## Introduction

In viticulture, soil properties seem to largely influence wine production in terms of quantity and quality (Maltman, 2013), as they are often indicated on wine bottles and are part of appellation schemes (Kuhnholtz-Lordat, 1963). Even though the influence of climate, biologic material and regional winemaking techniques on wine characteristics are widely accepted and scientifically demonstrated, there is an ongoing discussion about the contribution of grapevine mineral nutrition, and the potential effect of soil chemistry and geology (Bramley et al., 2011; van Leeuwen et al., 2009; Gonzalez-Barreiro et al., 2015; Maltman, 2008, 2013; Styger et al., 2011). Actually, the mechanisms involved in the soil-to-grape transfer of elements are complex and remain poorly understood even if there is an increasing interest of the scientific community in understanding the biogeochemical cycles of both nutrients and pollutants, as well as the biological and chemical signatures of terroirs (Vaudour et al., 2015).

45 One way of possible influence of soil chemistry on wine quality is plant nutrition and translocation of
46 elements through the plant (Maltman, 2013). Some 17 elements are essential nutrients for plant
47 functioning and are taken up from the soil (Marschner and Marschner, 2012). Concentrations of most
48 nutrients are closely regulated in plant tissues in a process called homeostasis (Marschner and
49 Marschner, 2012). By this self-regulation process (including particularly mineral nutrition, temperature
50 adjustment, transpiration function, etc.), a plant can maintain biological conditions and stability of its
51 dynamic equilibrium facing changes occurring in the environment (Castro et al., 2018). Mineral nutrients
52 play important roles in biochemical plant functioning as catalyzers, electron transporters or regulators of
53 osmotic pressure (Marschner and Marschner, 2012). However almost the whole periodic table of
54 elements can be found in plants and element concentrations vary systematically between different
55 wines (Almeida and Vasconcelos, 2001; Coetzee et al., 2014; Day et al., 1995; Greenough et al., 2005;
56 Kwan et al., 1979). For example, soil carbonate content is an important factor influencing plant
57 functioning, as certain nutrients are scarcely available (especially P and Fe) in carbonated environments
58 and plants have to deploy specific mechanisms to satisfy their needs (Marschner and Marschner, 2012;
59 Strom, 1997). Moreover, interaction among plant nutrients can involve antagonistic or synergistic effects
60 that potentially influence element efficiency in the plant system (Rietra et al., 2017). So, mineral
61 nutrition is a complex process and soil-to grape transfer mechanisms in vineyards are the result of
62 several interactions and processes, still poorly described (Likar et al., 2015).

63 Although differences in elemental contents of wines or grapes, likely do not have a proper taste, smaller
64 variations in element availability may influence the synthesis of compounds essential for grape maturity
65 and wine taste (Epke and Lawless, 2007; Sipos et al., 2012). For example the K/Ca equilibrium is
66 important for acidity in wine but K was also found to be important in polyphenol synthesis (Brunetto et
67 al., 2015; Daudt and Fogaça, 2008). Furthermore, many elements act as nutrients for fermenting yeasts
68 or catalyzers for synthesis of aromatic compounds (Pohl, 2007). Variations in metal ion contents have

been shown to influence grape properties as sugar and essential amino acid content in grapes, musts and wines (Pereira, 1988).

Mobility and phytoavailability of elements do not only depend on the soil content but are controlled by various soil properties such as pH, Eh, cation exchange capacity or organic matter content (Kabata-Pendias, 2004; Tyler and Olsson, 2001). Therefore, a thorough pedologic investigation is needed to identify soil properties controlling plant nutrition. Soil hydrological parameters have also been reported to widely influence mineral nutrition and fruit composition, as a resultant of soil-plant transfer (Ramos and Martínez-Casasnovas, 2006; Tournebize et al., 2012; van Leeuwen et al., 2009). Elemental contents of grapevine organs and their link with soil properties have been subject to several studies, some of them succeeded in identifying a direct link between soil concentrations or extractions whereas other do not (Angel Amoros et al., 2013; Cugnetto et al., 2014; Likar et al., 2015; Mercurio et al., 2014; Vazquez Vazquez et al., 2016). Only few studies have investigated grapevine nutrition on contrasted soils (Mackenzie and Christy, 2005; Peuke, 2000). In these studies differences in elemental contents and winemaking parameters have been identified (Mackenzie and Christy, 2005; Peuke, 2000). However, the vineyards investigated in these studies lie several kilometers apart, thus meteorological conditions were likely different, and no information is given on slope or exposition to sunlight. Thus, as it has been demonstrated that meteorological factors influence elemental compositions of grapevine (Boselli et al., 1998), a new perspective could be to work on the same climate parameters to better isolate the impact of elemental soil-to-grape transfers.

Besides elemental techniques, isotope ratios, and especially Sr isotopes, have been successfully used to determine geographical origin of wines, firstly studied by Horn et al. (1993) and more recently by various Italian, Portuguese or Canadian research teams (Martins et al., 2014; Petrini et al., 2015; Marchionni et al., 2013; 2016; Vinciguerra et al., 2016; Braschi et al., 2018). Actually, radiogenic Sr isotope ratios between $^{87}Sr$ and $^{86}Sr$ have been used to trace sources in geology and soil sciences for many years. Also

93 in vineyard environments Sr-isotope ratios have been used to support wine quality and guarantee good
94 traceability (Durante et al., 2018, 2015, 2013; Tescione et al., 2018). This is possible because stable Sr
95 isotope fractionation related to common low temperature reactions appears to be negligible compared
96 to source signature, also in biological systems (Blum et al., 2000; Capo et al., 1998). This makes Sr isotope
97 ratios a valuable tracer of the source of Ca nutrition, as the chemical behavior of the two elements is
98 extremely similar (Blum et al., 2000; Poszwa et al., 2000; Schmitt et al., 2017). This is especially
99 interesting when carbonates are involved in mineral nutrition of grapevine plants.

100 Moreover, recent studies have underlined the potential use of Cu isotope analysis in the context of
101 polluted agricultural soils (Babcsányi et al., 2016; Fekiacova et al., 2015) and their help in determining
102 the mechanisms of Cu mobility in soils (Blotevogel et al., 2018) as well as the mechanisms of elemental
103 transport towards plants or trees (Mihaljevič et al., 2018). The discussion on Cu isotope fractionation
104 induced by plants is still ongoing, but first results reported that Cu isotopes fractionate considerably
105 during uptake and translocation: they have been recently used to identify Cu uptake mechanisms (Jouvin
106 et al., 2012), including reduction at root surfaces and preferential translocation of light isotopes to
107 higher foliar levels (Weinstein et al., 2011). Diverging results from different growth settings also suggest
108 that fractionation of Cu isotopes depends on environmental conditions (Jouvin et al., 2012; Li et al.,
109 2016; Ryan et al., 2013; Weinstein et al., 2011). Cu isotope analysis is thus an interesting tool to
110 investigate Cu mobility in vineyard environments.

111 The present study aims at investigating soil formation and mineralogical as well as geochemical
112 differences occurring between two adjacent plots in the Soave area (Veneto, Italy), using complementary
113 techniques. Because different bedrock types underlie the soils of the two plots, the study of the
114 pedological characteristics and of the elemental distribution along the soil-to-grape continuum will allow
115 us to establish a link between soil properties and plant composition under the same metereological and

agronomic conditions. In particular, the use of Sr and Cu isotopes will help to better identify the biogeochemical processes and elemental transfers occurring in this vineyard soil-plant system.

## Materials and Methods

### Area of study

The study was performed in the Cantina Filippo Filippi domain, in the Castelcerino wine growing area, in the Soave appellation (45.464911 N, 11.236905 E). The Soave vineyard is located in the southern foothills of the Alps, in Northern Italy, in the Veneto region. Geologically, the studied site lies between different bedrocks: basalts and volcanic tuff mainly in the Alpone valley and limestone in the western parts of the appellation area (Benciolini et al., 2006). Volcanic rocks come from tertiary volcanic activity during the alpine orogenesis with the closest eruptive centers in Alpone valley and north of Cazzano di Tramigna village (De Vecchi et al., 1976). Limestones are from paleogenic and lower Miocene but siliclastic marine sediments and marls are also found in the area as some parts of the Lessini shelf became emerged in early Oligocene whilst others remained on the slope of Thetys ocean (Bassi and Nebelsick, 2010; De Vecchi et al., 1976). Basalt outcrops are mainly found to the northeast, tufa to the north and west and limestones in the south and west of the vineyard (Figure 1).

The plots are cultivated with the typical Garganega cultivar in organic viticulture by the same vine grower. Treatment, pruning and harvesting intervals differ only by days and treatment amounts are the same on both plots. Both plots are in viticulture for 65 years. Plant material is still the first generation planted thus no deep ploughing occurred since the beginning of cultivation. Vineyard management has been organic for the last 12 years and grapevine plants are irrigated in case of severe droughts. The soil between grapevine rows is grass covered.

138

139 **Field pedological description**

140 Soil profiles were studied along two catenas within the two studied parcels (Figure 1), following the main
141 slope. Soil profiles descriptions and pedological investigations were performed both through soil pits
142 until a depth of 50-60 cm for a more complete surface description and an Edelman soil corer was used
143 down to the depth of 120 cm maximum for subsoil study. Structure, texture, roots abundance, biological
144 activity and pedological features (e.g., mottling, coatings, secondary phases precipitations, root and
145 pores distributions) were described directly on the field (i.e., at field moisture). Soil structures below 50
146 cm depth are indicative structures as structure observation is biased during soil corer sampling. Colors
147 were determined using a Munsell color chart in the year 2000 revised version (Munsell, 2000). The
148 occurrence of carbonate phases and their types (primary versus secondary carbonates phases) was
149 established using 1 M HCl (effervescence method). Samples for bulk densities of surface horizons of B60,
150 B150, C60 and C155 were taken by the cylinder method. Soils were classified according to the World
151 Reference Base for soil resources from FAO/ISRIC/ISSS, 2014 (2015 update).

152

153 **Hydrological and geomorphological properties**

154 As reported by van Leeuwen et al. (2009), vine water status and especially water deficit stress are key
155 factors of mineral nutrition and grape composition. Among the various methods largely employed to
156 assess the hydric stress, stable isotope ratio in carbon ($\delta^{13}C$) are reported to be highly significant (Ramos,
157 2017; Ramos and Martínez-Casasnovas, 2006; Tournebize et al., 2012; van Leeuwen et al., 2009).

158 $\delta^{13}C$, the $^{13}C/^{12}C$ ratio expressed relative to the Pee Dee Belimnite standard (PDB), has been measured as
159 an integrative indicator of water status of grapevine plants. As explained by Farquhar et al., 1989 , $^{12}C$ is

preferentially taken up by the enzymes involved in photosynthesis and « isotope discrimination » between air and plant occurs. In water stress conditions, this discrimination is less severe and plants contain more $^{13}C$ compared to those produced when plant water status is not limiting. Van Leeuwen et al. (2009) linked $\delta^{13}C$ ratios in grapevine plants to stem water potential, sugar content and acidity. That article also defines threshold values of no water stress ($\delta^{13}C < -27$ ‰) and severe water stress ($\delta^{13}C > -20$ ‰). However, it was reported that $\delta^{13}C$ values are dependent on grapevine variety (Gómez-Alonso and García-Romero, 2009). In this study, $\delta^{13}C$ have been calculated with $^{13}C/^{12}C$ values measured on ground leaf and grape samples, on an Isoprime 100 IRMS by Elementar® according to the Equation (1):

$$\delta^{13}\mathrm{C} = \left( \frac{\left(^{13}C/^{12}C\right)_{Sample}}{\left(^{13}C/^{12}C\right)_{PDB}} - 1 \right) * 1000 \qquad \text{Equation (1)}$$

Hydric stress occurs when the soil is dry enough, and thus the rate of flow of water out of the soil is a key determinant on the occurrence of water deficit stress. The first order controls on the rate of drainage of soils are their hydraulic conductivity and the topographical slope: the higher they are, the faster will be the drainage. Here, hydraulic conductivity at saturation was estimated by infiltration tests at constant hydraulic head (Porchet and Laferre, 1935) in 45 cm deep standardized boreholes for the different sampling points from C and B catenas, as already reported by Blotevogel et al. (2018).

Moreover, in order to estimates slope distributions, the studied vineyard was mapped using a kinetic differential GPS and an elevation map grid was calculated by kriging between 47968 data points using Surfer 13 software package to propose a vector map indicating slope direction.

All these parameters allow a characterization of the two vineyard plots in terms of their hydrological and geomorphological behaviors.

182 **Sampling of soils, plants and rocks**

183 Soil sampling was performed following the two catenas identified in Figure 1: "B" (basalt) catena for soils
184 over basaltic bedrock (in blue) and "C" (carbonate) catena for soils over calcareous bedrock (in red). The
185 numbers identifying each sampling spot correspond to the distances in meters from the gravel road on
186 top of the parcels. Rock samples of limestone, tufa and basalt were collected from the respective
187 outcrops denoted in geological maps of the Soave region and described by Benciolini et al. (2006), and
188 marked in Figure 1. Limestone outcrops are situated within the C catena, basalt outcrops are found uphill
189 from the B catena and tufa outcrops uphill from the C one. This sampling strategy aimed at determining
190 an endmember of each parent material to study pedogenetic mechanisms occurring in this area.

191 Leaves and grapes were sampled at the end of September (2015), just before grape harvest, as
192 composites from 5 plants surrounding the soil sampling site. Only tissues that visually appeared healthy
193 were sampled at chest height (~ 150 cm from soil) using a ceramic knife. Leaves were washed three
194 times in ultrapure water and thereafter frozen and freeze dried. Grapes were sampled including the
195 pedicel and rinsed with ultrapure water and subsequently freeze dried. Plant samples were ground
196 under liquid nitrogen using an agate mortar.

197

198 **Soil physico-chemical properties**

199 Soil samples were air-dried for several days under a laminar flow hood and sieved to 2 mm. Soil pH was
200 measured on 1 g in ultrapure water (18.2 MΩ) following ISO 11464 protocol. The cation exchange
201 capacity (CEC) was measured according to the cobalthexamin method, described by Orsini and Remy
202 (1976), Ciesielski and Sterckeman (1997) and Arrouays et al. (2011): 1 g of soil was shaken in 20 mL of a
203 0.017 mol $L^{-1}$ cobalthexamine solution during 1 h, solutions were subsequently centrifuged and
204 supernatant filtered at 0.22 µm. Then cobalthexamine loss from solution was determined by absorbance

loss at 475 nm with a Varian Cary 50 spectrophotometer. Soil Organic Carbon and Soil Inorganic Carbon (respectively SOC and SIC) were calculated after subsequent measures of raw and calcined samples on a Horiba EMIA – 320V CS automate, according to the method reported in Bao et al. (2017), Blotevogel et al. (2018) and Kania et al. (2019). For granulometric analysis, 2 g of soil samples were suspended in distilled water and sieved to 500 µm. The fine fraction was subsequently treated with 10 mL hydrogen peroxide to remove organic matter. Treatment was repeated until no foam or gas formation was observed when adding $H_2O_2$. Samples were treated with an acetic acid/ammonium acetate buffer at pH ~4.5 to eliminate carbonates phases. Treatment was then repeated until no effervescence was visible. Finally, samples were washed in ultrapure water and grain size distribution was measured on a Horiba LA-950 laser diffraction granulometer, as reported by Wanogho et al. (1987). Soil bulk densities were determined after soil drying at 105°C during 48h (until constant mass is reached).

**Mineralogy of rock and soil samples**

Rock samples were washed with ultrapure water. Approximately 200 g of sieved soil samples (<2 mm fraction, i.e., fine earth) and rock samples were crushed using a planetary mill made from agate. X-Ray Diffraction (XRD) spectra were acquired directly using an INEL diffractometer equipped with a CPS 120 detector at 40 kV and 25 mA applied to a Co anticathode (λKα=0.179 nm; λKß=0.162 nm) for crushed soil samples and a Bruker D8 advance at 40 kV and 40 mA applied to a Cu anticathode (λKα=0.154 nm; λKß=0.139 nm) for crushed rock samples. The crystallized compounds were identified through the comparison with the COD 2013 database. Clay type was identified on oriented thin sections using the <2 µm fraction of decarbonated soil samples. Oriented thin sections were measured as natural sample, heated to 550°C for two hours and treated with ethylene glycol. Diffraction spectra were then measured using the Brucker D8 device with the setting described above.

228

229

230 **Elemental contents in rock, soil and plant samples**

231 For total elemental content analyses, 100 mg of each crushed soil or rock sample were digested in a CEM
232 MARS 5 microwave oven using ultrapure acids (9 mL $HNO_3$ : 2mL HCl : 3mL HF). For each digestion run,
233 an experimental blank and a standard (SRM 2709a or BCR-2) were included. Ground plant samples (200
234 mg) were digested in a CEM MARS 5 microwave oven using suprapure acids (10 mL $HNO_3$ : 3mL HCl :
235 0.2mL HF). For each digestion run, an experimental blank and a standard (SRM 1515) were included.

236 After acid digestion, element contents were measured with an Agilent® 7500ce ICP-MS at the GET
237 laboratory in Toulouse and leaves with an iCAPQ Thermo Scientific at Hydrosciences in Montpellier using
238 an In-Re internal standard to correct data for instrumental drift and plasma fluctuations. Ca, Mn and Fe
239 contents in soil samples were measured using an ICP-OES Horiba ultima 2. Element concentrations were
240 expressed in dry weight (mg $kg^{-1}$, DW). Quality and measurement traceability were ensured by
241 measuring replicates of SLRS-5 river water standard. N content of leaves was measured during C-isotope
242 analysis Isoprime 100 IRMS, as described above for C.

243

244 **Sr isotope analysis**

245 From the above described sample digests, aliquots were taken to contain 300 ng of Sr. They were
246 dissolved again in 0.5 mL of 2M $HNO_3$ and added to a column containing 150 µl of Sr-Specific resin. The
247 matrix was eluted using 0.4 mL of 2M $HNO_3$ followed by 1.5 mL of 7 M $HNO_3$ and another 0.3 mL of 2 M
248 $HNO_3$. Strontium was then recovered in 1 mL of 0.05 M $HNO_3$. All acids used for purification were double
249 sub-boiled prior dilution. Samples were evaporated to dryness and deposited on W-filaments.

Measurements of Sr isotope composition were carried out on a Thermo® Triton thermal ionization mass spectrometer (TIMS). NBS 987 standards were run to verify the precision of the method. As differences in Sr isotope ratios are mostly radiogenic (from $^{87}Rb$ decay), Sr-isotope ratios are expressed as ratios between $^{87}Sr$ and $^{86}Sr$.

**Cu isotope analysis**

For Cu isotope analyses, aliquots of digested samples containing 500 ng of Cu were purified using anionic AG MP-1 resin. Separations were carried out at least twice per soil sample (elution with HCl and $H_2O_2$) using AG MP-1 resin with Biorad® column, according to the protocol adapted from (Maréchal et al., 1999) and detailed in Blotevogel et al. (2018). Recovery was checked to be 100 ± 5% and BCR-2 standards were run to assure result quality. Our measured values (0.21 ± 0.03 ‰) are in line with formerly published values of 0.20 ± 0.10 ‰ (Babcsányi et al., 2014) and 0.22 ± 0.05 ‰ (Bigalke et al., 2010a). Purified solutions were spiked with IRMM Zn standard for measurements on MC–ICP-MS (Nu Plasma 500, Nu Instruments® at ENS in Lyon; Neptune plus, Thermo Finnigan® at GET in Toulouse). Exponential laws were used to correct for mass bias using 66/64, 68/64 and 68/66 Zn isotope ratios (see Maréchal et al. (1999) and Blotevogel et al. (2018) for more details). Cu isotope ratios are expressed in ‰ relative to NIST 976 Cu standard, according to the Equation (2):

$$Equation\ (2) \qquad \delta^{65}Cu = \left( \frac{\left(^{65}Cu/^{63}Cu\right)_{Sample}}{\left(^{65}Cu/^{63}Cu\right)_{NIST976}} - 1 \right) * 1000$$

**Results**

**Field morpho-pedological description and soil identification**

Studied soil profiles from the C catena feature granular to fine subangular blocky soil structure with worm casts on top of the soil profile (i.e., A horizon, 0-10 cm). The structure evolves to blocky angular in intermediate calcic horizons, whereas the deepest calcic soil horizons seems to display single grained structure for C220 and powder-like structure in C155 (soil structure estimate using soil corer). Only C60 displays a more massive/prismatic structure in subsoil horizons. The texture is loamy clayey on topsoils and gets coarser towards the bottom. Soil colors are mostly 10 YR 4/3 but the lowest horizon of C220 displays 10 YR 5/3 colors. All studied soil profiles from the C catena present an increase in carbonate content with depth, as indicated by their reaction with 1 M HCl. The increase in carbonate phase content with depth is due to two main processes: i) primary carbonate dissolution in surface horizons; and ii) secondary carbonate formation in subsoil. The soils from the C catena were identified as Cambic Calcisols (according to the World Reference Base for soil resources from FAO/ISRIC/ISSS, 2014), as described in Figure 2.

Soil profiles from the B catena also show granular to subangular blocky structure within the first 10 cm. The intermediate and deepest horizons investigated generally display angular blocky structures or quasi massive soil structure. Indeed, cambic horizons located beneath 30 cm depth present massive structure when humid and show wedge-shaped aggregates and shrink-swell cracks when dry suggesting vertic properties. However, the deepest horizon of B60 seems to features a single grained structure and the two deepest horizons of B150 have powder-like to more aggregated structure (supposed blocky angular). Texture varies from loamy clayey in topsoil horizons to clayey in protovertic horizons. Again, the bottom layer of B60 differs from the rest of the studied soil profiles being clayey-loamy-sand and thus much coarser. Colors are darker than calcisols from the C catena (mainly 10 YR 3/2 and 10YR 2/1). Only B60 bottom layer is brighter with 10 YR 5/6. The occurrence of shrink swell cracks and wedge shaped aggregates was established for most of the subsoil horizons after 30 to 40 cm depth. However, those structures resulting from shrinking and swelling properties of clays are not considered as currently active

because of a quasi-constant humidity all year long (climate with no dry season and irrigation) so that vertic properties are poorly expressed at the soil profile scale. A secondary precipitation of carbonate phases was observed at various depth along the soil profile (see Figure 2) suggesting protocalcic properties within these soils. Colluvic material was only established for B150. B20 and B60 were identified as Vertic Cambisols protocalcic whereas B150 was identified as a Vertic Cambisol colluvic (WRB soil classification), as described in Figure 2.

**Vineyard hydrological and geomorphological properties**

The results of soil hydraulic conductivity are reported in Table 1. The soil permeability K is slightly lower in vertic soils ($8 \times 10^{-7}$ to $10^{-5}$ m $s^{-1}$) than in calcareous ones (1 to $7 \times 10^{-5}$ m $s^{-1}$). The lowest hydraulic conductivity is measured where the infiltration test depth includes the vertic horizon. However, these values remain close, suggesting that the soil hydraulic properties are quite the same between the two vineyard plots.

Moreover, results of $\delta^{13}C$ measurements (Table 3) show no significant difference between the two plots (B or C catena). The measured $\delta^{13}C$ values ranging between -26.30 and -27.64‰ and -24.27 and -25.82 for respectively the leaves and the grapes from the 2 plots are in the upper range of the thresholds defined by van Leeuwen et al. (2009) for water deficit. This suggests that the plants did not suffer severe water stress and that there is no significant difference in water stress between the two plots (Table 3; non-parametric Mann-Whitney U-test: p-value=0.5 and 0.35 for leaves and grapes, respectively).

Concerning geomorphological properties, the vector map indicating slope direction is presented in Figure 3. Elevation of the vineyard plots is the highest in the north east and the lowest in the south west. There is no strong variability of slope between the two vineyards, since the variation of elevation are mainly related to localized, steep banks rather than through distributed and strongly variable sloping.

318

319 **Mineralogical and physico-chemical properties of soils**

320 The mineralogical and physico-chemical characteristics of the soil samples are summarized in Table 1.

321 The mineralogy of parental rocks and soils is reported in the XRD spectra of Figure 4. The XRD spectra of
322 limestones taken from the outcrops between the parcels exclusively show calcite peaks. The tufa
323 samples also contain the peaks typical of calcite, but also exhibit peaks of clay minerals identified as
324 smectites (Figure 4b). Only the basalt samples have more complex mineralogy (Figure 4a) containing
325 albite, titanite, chabazite and diopside. In most soils of the C catena calcite remains the main mineral.
326 Only in the topmost horizon of C60, quartz is the major phase (examples of diffraction spectra are shown
327 in Figure 4). In all soils, peaks belonging to smectite-type minerals are detected and clay mineralogy
328 appears to be the same (i.e., montmorillonite type smectite) in both catenas according to orientated thin
329 section analysis (data not shown). Furthermore, albite and titanite peaks are present in C60 and C155.
330 Diffraction patterns for soils of the B catena show the same minerals phases as basaltic rock, except
331 chabazite. Smectite is detected in all of those soils and some horizons show calcite. The presence of
332 calcite was expected as the vineyard was irrigated in case of need. In the lowest horizon of B60, calcite is
333 more abundant than the two other minerals. In B60 50-70 cm, quartz is found to be the most abundant
334 mineral.

335 All studied soil horizons have pH values higher than 7 (Table 1). The lowest pH values within a soil profile
336 are systematically found in topsoils and ranges from 7.2 in C60 and C220 to 7.5 in B20. The pH values of
337 subsoils vary between 7.6 in B150 (40-50 cm), C60 (30-50 cm) and C155 (10-50 cm). The highest pH value
338 is 8.1 and was measured in the deepest horizon of C220. Cation exchange capacity is around 80 cmol $kg^{-1}$
339 in most horizons. However, the deepest horizons of B150 have slightly lower CEC with values of 70.0 and
340 72.2 cmol $kg^{-1}$, whereas the soil C220 has the lowest CEC with values between 66.0 cmol $kg^{-1}$ in the

topsoil and 55.8 cmol $kg^{-1}$ in the lowest soil horizon. The soil C220 is also the soil with the highest inorganic carbon contents comprised between 3.7% in the topsoil and 5.6% in the lowest soil horizon. Inorganic carbon contents of around 2% (wt) are measured in the deepest horizon of C60 and the two deepest horizons of C155 alongside with the two topmost horizons of B20 (Table 1). Values between 1.4 and 1.6% are measured in the two upper horizons of C155 and the lowest horizon of B60. All other horizons have inorganic carbon contents of less than 1%. Organic carbon contents decline in all soil columns with depth. Organic carbon contents in topsoils ranges from 7.1% in B60 (0-10 cm) to 2.0% in C155 and systematically declines to < 0.1% in the lowest soil layers. Only B20 (110-120 cm) and C220 (50-60 cm) contain measurable amounts of organic carbon (0.8 and 0.2% respectively).

Granulometric analyses after carbonate removal show that most of the soil horizons have similar granulometric distribution, characteristic of silty clay to silt-clay-loam textures (Figure 5): between 30 and 40% of clay and very little sand (generally <10%). Higher clay contents are found in the soil B150 as well as the topsoil of C60 that (about 50%), which can be classified as having a heavy clay texture. The lowest clay contents are found in lowest horizons of B60 and C155 (15 and 10 %, respectively) and horizons of C220 have slightly lower clay contents (24-28 %). The soils from the C catena have slightly higher sand contents than the soils from the B catena. The highest sand contents of 11 to 19% are found in B60 (70-90 cm), C155 (50-70 cm) and C220 (20-50 cm).

Surface A horizon from both catena soils display very low bulk density values from 0.7 to 1, in accordance with the intense biological activity (abundant worm casts) observed in the first ten centimeters of the soils. Bulk densities for the $B_{ik}$ horizons of the B catena soil profiles are relatively low with values from 1 to 1.2 in accordance with the vertic properties of these soils, implying low bulk density during humid periods. Indeed, the volumetric water contents of the samples were estimated at approximately 40 to 50% during the sampling campaign. Subsurface horizons from the C catena show higher bulk densities values from 1.2 to 1.7.

365

366 **Elemental contents in rocks and soils**

367 The results of elemental contents in rocks and soils are reported in Table 2. The elemental
368 concentrations of the major elements Mg, K, Ca and Mn in the basaltic rock (44.2, 9.9, 55.3 and 1.25 g kg$^{-1}$
369 respectively) are within the range of values found in other studies in the area (De Vecchi et al., 1976).
370 Conversely, we find contents of Fe, Al and P that are 1.5 to 2 times higher than reported in the literature
371 (De Vecchi et al., 1976). Concentrations of all measured elements except Ca (394 g kg$^{-1}$) are relatively low
372 in the limestone. Especially, the content of the transition metals Mn (0.67 g kg$^{-1}$), Fe (3.32 g kg$^{-1}$), Cu
373 (2.57 mg kg$^{-1}$) and Zn (3.81 mg kg$^{-1}$) is low compared to the basalt (1.25 and 81.9 g kg$^{-1}$ respectively for
374 Mn and Fe, and 49.1 and 120.4 mg kg$^{-1}$ for Cu and Zn). Molybdenum is the only element besides Ca that
375 is more concentrated in the limestone (0.25 mg kg$^{-1}$) than in the tufa (0.17 mg kg$^{-1}$), but still less
376 concentrated than in the basalt (1.10 mg kg$^{-1}$).

377 The tufa rock concentrations of elements are intermediate between those of basalt and limestone for
378 most elements. Ba, Cu, P and Al have almost identical concentrations in the tufa as in the basalt, whereas
379 all other elements are more concentrated in the basalt. In basaltic rocks, the most abundant element
380 measured is Fe, in contrast to tufa and limestone where Ca is far more abundant. In soil profiles, Ca and
381 Fe are the most abundant elements in the order of hundreds of grams per kg of bulk soil. Some of the
382 elements show distinct variations with depth. This is the case for Cu and S which are much more
383 concentrated in the top of the soil columns. However, also K, Zn and, to some extent P, show increasing
384 concentrations in the top of the soil profiles. For Ca the trend is inversed, with higher concentrations in
385 the bottom horizons of the soils, especially on catena C. Other elements are more or less equally
386 distributed through the soil profile. Magnesium is depleted in the top soil horizons of B150 and C60.
387 There are few significant differences in elemental content between catena B and catena C. One sided

388 non-parametric Mann-Whitney U-test performed over all soil horizons of the respective plot, that Ca and
389 Ba contents are significantly higher in C catena soils. On the other hand significantly higher
390 concentrations in the B catena were detected for Mn, Fe, Sr and Mo.

391

392 **Elemental contents in leaves and grapes**

393 Elemental contents in leaves of both catenas are of the same order of magnitude (Table 3). However,
394 some significant differences identified using a Mann-Whitney U-test. K and Zn concentrations in leaves
395 of the C catena are higher than those in the B catena, whereas Sr concentrations are higher in leaves
396 from the B catena. No significant differences were detected for other elements contents in leaves. The
397 values measured are around average contents reported in the literature for Mg, P, Mn and Zn
398 (Marschner and Marschner, 2012). Cu and Ca contents (75 mg $kg^{-1}$ and 32 g $kg^{-1}$, respectively) are higher
399 compared to the corresponding values of 6 mg $kg^{-1}$ and 5 g $kg^{-1}$ reported in literature. Nitrogen, K and Fe
400 concentrations are low, with respectively, 14.3 g $kg^{-1}$, 7.2 g $kg^{-1}$ and 43.7 mg $kg^{-1}$, relative to literature
401 values of 23-43 g $kg^{-1}$, 10 g $kg^{-1}$ and 100 mg $kg^{-1}$ (Grechi et al., 2007; Marschner and Marschner, 2012).

402 For grapes, the elemental contents are consistent with the literature (Cugnetto et al., 2014; Scherz and
403 Kirchhoff, 2006). However, comparison to most sources is difficult due to different sampling strategies
404 (including pedicels, juice only etc.) and differences in notation (dry matter vs. fresh weight) (i.e. Almeida
405 and Vasconcelos, 2003; Bertoldi et al., 2011). Significantly higher concentrations of K, Al and Mo are
406 found in the C-catena whereas Ca and Sr concentrations are higher in grapes from the B-catena.

407

408 **Sr and Cu isotopes in the soil-plant continuum**

Isotope ratios for Sr and Cu are reported in Table 2 for soils and rocks, and in Table 3 for plant leaves. Cu-isotope ratios could not be measured in grape samples because of the low concentrations of Cu in this plant compartment and the interference of residual organic matter with the separation protocol.

Strontium isotope ratios are the highest in limestone with $^{87}Sr/^{86}Sr$ of 0.7070. Sr isotope ratios are equal to 0.7032 in basaltic rock and 0.7067 in tufa rock, closer to limestone. Moreover, in soils as well in leaves, Sr isotope ratios are always higher in samples from the C catena than in those of the B catena. This difference is significant using a Mann-Whitney U-test.

Copper isotope ratios in soils were already published in Blotevogel et al. (2018), see there for more details. Within the same soils, the values vary slightly but significantly between different soil types though 2SD interval overlap. If we discard the B60 70-90 horizon for being obviously calcareous, the p-value (Wilcoxon Rank Sum test) is <0.002 comparing mean isotope ratios of 0.18‰ for calcaric cambisols and 0.28‰ for vertic soils. The B60 surface horizon contains the heaviest measured Cu signature for soil samples present vineyard (i.e., 0.37 ± 0.05‰). This is also the horizon containing the most Cu and organic carbon, suggesting an organo-complexation of Cu with humic acid, as already suggested by Bigalke et al. (2010b) and Blotevogel et al. (2018). The lowest isotope ratio is found in the deepest horizon of B60 (0.12 ± 0.04‰). That horizon contains a considerable amount of inorganic carbon (1.6%), and calcite is the most abundant C-bearing phase. In plant leaves, Cu isotope ratio varies more than in soil samples, varying from -0.86 to -1.83 for leaves of vine plants taken respectively in C155 and C60 soils.

## Discussion

### Influence of geology *versus* pedogenetic processes on soil properties in the Soave vineyard

In former studies of the Soave vineyard, only the presence of limestone and volcanic rocks was highlighted (Benciolini et al., 2006). However the presence of tufa rocks fits into a greater geological context with variations in land and ocean levels that left behind a variety of calcareous and siliclastic rocks in the Lessini mountains (Bassi and Nebelsick, 2010; De Vecchi et al., 1976).

As explained above, hydrological and geomorphological properties appear to be similar between the two vineyards plots, as suggested by the values of soil hydraulic conductivity (Table 1 and $\delta^{13}C$ measurements in leaves and grapes in Table 3). Even though there are slight differences in hydraulic conductivity, plants do not suffer severe water stress and especially there are no significant differences in $\delta^{13}C$ measurements between plants from the two plots. Thus hydraulic parameters were considered of no influence in our study, and their impact was not investigated in terms of soil-to-grape transfer of nutrients and pollutants.

According to our dataset, the soils of the two catenas are clearly dissimilar after field pedological description in terms of morpho-pedological features. Color, structure and inorganic carbon content show distinct features of the two soil types. There is a tendency for more massive or prismatic structures associated with shrink swell-crack features in the B catena (depending on water content) and more polyhedral to single grained structures in the C catena. Furthermore, soils of the C catena show important calcic properties with calcic horizons lighter in color and in secondary carbonates contents, and all cambic calcisol horizons show traces to large amounts of calcite in XRD spectra. Even if secondary calcite phases are found in soils from the B catena, the studied Vertic Cambisols clearly have minerals inherited from basalt, have greater amount of clay fraction and display vertic properties (shrink swell cracking, wedge shapes aggregates, slickensides type features). Besides, soils from the C catena tend to have higher sand contents even after elimination of carbonates. However, a more detailed look also shows similarities. There are several calcic horizons in the upslope soils of the B catena and CEC values are similar in all soils; only C220 shows lower CEC values than the other soils and pH values are >7 in all

455 horizons. This is attributable to a control of carbonate phases on soil pH in all soils. The chemical
456 composition of the soils is also surprisingly similar. The only difference is the higher Ca contents in
457 carbonated horizons whereas the contents in metals such as Al, Mn and Fe are relatively high in all soil
458 samples. The C220 soil contains more Ca and less transition metals than the other soil profiles, indicating
459 that this soil is less influenced by basaltic material than all other soils. All soils seem to have formed
460 under mixed influence of the three bedrocks present in the study area.

461 In the C catena a distinct increase in Ca content with depth as well as the increase in relative importance
462 of the calcite peaks in XRD spectra indicate that carbonate weathering is one of the soil forming
463 processes involved in this catena (Figure 4). However, the relatively high metal and smectite contents as
464 well as the increase in Al/Fe ratios in soils compared to limestone indicate that limestone weathering is
465 not the only soil forming process. The influence of the tufa rock weathering would possibly explain these
466 observations and is supported by the $^{87}Sr/^{86}Sr$ values close to tufa and limestone rocks in the soils of the
467 C catena. Besides, soils of the C catena mainly in more upslope positions contain trace of feldspars and
468 titanite typically inherited from basaltic rock (Figure 4). The presence of minerals inherited from the
469 basalt indicates that there is at least some contribution of basalt to the soils from the C catena.

470 The soil forming processes along the B catena are also complex. The finer texture of soils downslope
471 (B150) indicates that erosive transport (colluvic processes) occurs. The presence of calcic horizons
472 together with non-calcic horizons in upslope soils (B20 and B60) indicates an influence of limestone
473 through erosion processes (particulate transport) or secondary carbonate precipitation implying the
474 circulation of water charged with Ca and dissolved carbonate species. The presence of quartz also
475 confirms an erosive contribution from sedimentary rocks.

476 Copper and S contents decrease with depth within the soil profiles, which is likely due to fungicide
477 treatment. XRD analyses on oriented thin sections indicate no difference between smectite types from

478 the B and the C catena (data not shown). This suggests that all soil smectites formed under the same
479 conditions, possibly through basalt weathering. Some contribution of inherited smectites from tufa rock
480 weathering during pedogenesis is expected in catena C. Therefore, such inherited smectites entrapped in
481 the tufa rocks might have formed from past basalt weathering, which is still occurring in this area. Tufa
482 rocks seem to have an important role in pedogenesis of the studied soils.

483 A mixing diagram (Figure 6) was drawn using the contents of Ca and Sr and the $^{87}Sr/^{86}Sr$ ratios of the
484 three bedrock types to illustrate their influence on the composition of the corresponding soil horizons
485 and grape leaves (see Langmuir et al., 1978, for details on mixing diagram interpretation). Almost all soil
486 horizons lie outside of the mixing triangle as a decrease in Ca/Sr ratios is expected during weathering
487 (e.g. Pett-Ridge et al., 2009). The C220 horizons lie on the mixing line between the limestone and the
488 tufa with decreasing Ca/Sr ratios towards the surface. The $^{87}Sr/^{86}Sr$ ratios are unchanged compared to
489 the limestone bedrock, as already observed for various soils from typical bedrock endmembers (Braschi
490 et al., 2018). In our case, this observation confirms that weathering of limestone is a major soil forming
491 process for the C220 soil. In addition, for the two topmost horizons of C60, the $^{87}Sr/^{86}Sr$ ratios are in the
492 range of values measured in tufa and limestone. Their shift towards lower Ca/Sr values indicates that
493 weathering of one or both of these rocks played a role in their formation. For the other horizons, the
494 $^{87}Sr/^{86}Sr$ values differ from all bedrocks indicating a mixed influence of bedrocks. The deeper horizons of
495 C60 lie together with the C155 horizons and rather close to the $^{87}Sr/^{86}Sr$ values of tufa and limestone,
496 indicating a major influence in their formation by those rocks. If they were derived mainly from the tufa
497 bedrock, weathering played a minor role in their formation as Ca/Sr values are not far from those of tufa
498 rocks. If the main source material was limestone, weathering in those horizons was even stronger than in
499 C220 horizons. A basalt influence is also a possibility to explain the observed soil signatures. It would be
500 coherent with the presence of mineral phases from basalt such as titanite in the soils from the C catena.

Isotope ratio $^{87}Sr/^{86}Sr$ values of all B catena horizons align between the basalt pole and a pole with lower Ca/Sr ratio and higher $^{87}Sr$ signature than tufa and limestone (Figure 6). We suggest this pole corresponds to secondary carbonate formation in basaltic soil. B150 soils are closest to the basalt pole. Whereas B20 and B60 that were more strongly influenced by carbonate rocks and secondary carbonates have higher $^{87}Sr/^{86}Sr$ values. This illustrates the complex interplay between at least three parental rock sources and pedogenetic processes (weathering, secondary phase precipitation, erosive transport) in the area. Erosive transfer, pedogenesis and complex bedrock geometry make the vineyard zones less clearly distinct in their biogeochemical properties than expected from macroscopic pedological observations.

**Influence of soil characteristics on plant elemental content**

The complex pedogenetic processes in the Soave soils have, to a large extent, homogenized elemental contents of bulk soils even though structure and color are clearly different according to field observations. A dominant influence of bedrock chemistry on soil chemistry is visible only for few elements. One remaining difference is the Ca content as marker of the degree of carbonate content. The increase of Ca contents with depth in the C catena reveals a weathering gradient within the soil column, underlining the fact that those soils have not been deeply ploughed recently. The presence of carbonates is an important control on pH and thus on the mobility of elements (Kabata-Pendias, 2004). Cu and S contents decrease with depth within the soil profiles. Such decrease is due to progressive migration of those elements, which are frequently used in plant protection especially in organic viticulture (Blotevogel et al., 2018). The gradients of nutrients K, Zn and P come more likely from the uptake at depth by the plants and deposition through litter fall (Jobbagy and Jackson, 2001). The fact that Mn, Fe, Sr, Mo and Ba are more concentrated in soils from the B catena is related to their higher abundance in the basaltic bedrock.

On the mixing diagram (Figure 6), leaves from different catenas display different $^{87}Sr/^{86}Sr$ values. Leaves from the B catena have values that are significantly lower than tufa and limestone rock indicating an influence of basalts on their Sr-uptake and thus on Ca-nutrition as Sr is considered as an analog of Ca, interchangeable in plant growth (Walsh, 1945). Plants from C catena all have Sr isotope ratios in the range of tufa or limestone. Leaves from C155 and C220 also have higher Ca/Sr ratios than the leaves from the B catena. This shows that, even in a context where plants are influenced to different degrees by the same rock formation, the geological origin of their nutrition can be traced using alkaline earth elements.

Among the vine leaf samples, Cu contents are high (from 34 to 125 mg $kg^{-1}$) in comparison with the literature (Ko et al., 2007; Chopin et al., 2008) and large variations are observed. These variations cannot be explained by variable soil Cu contents. The highest leaf Cu contents are measured in the upslope sampling sites. Nevertheless, a clear link between Cu concentration and Cu isotope ratios is observed: the higher the leaf content of Cu, the lighter the Cu isotopic composition (Figure 7). Isotopic ratios are much lighter in leaves (-0.9 to -1.8‰) than in soils or pesticides (-0.49 to 0.89‰) reported in Blotevogel et al. (2018). As a consequence, incomplete washing can be excluded as a source of the high Cu contents. This points towards a control of Cu content and isotopic ratios by physiological processes. Weinstein et al. (2011) suggested that the translocation of Cu to higher plant organs induce light isotope fractionation. In this study, an equation linking the leaf height (from the soil) to the isotope ratios was proposed. This equation predicts surprisingly well (calculated $\delta^{65}Cu$ = -1.57‰) the isotope ratios measured in the field-grown grapevines (-0.9 to -1.8‰). However, isotope fractionation within plants is still under discussion. Jouvin et al., (2012) reported that light Cu was taken up from a nutrient solution and light Cu isotopes become further enriched in aerial parts of the plants. On the contrary, another study reported uptake of light Cu to roots and subsequent heavy Cu enrichment in aerial parts (Ryan et al., 2013). The last study used extreme conditions with high doses of ionic Cu likely not occurring in nature. Light isotope

548 enrichment with height has also been reported for the chemically similar element Zn (see Caldelas and
549 Weiss, 2017 for a review and discussion of potential mechanisms). For Zn it was also reported that
550 transpiration flow controls root to shoot Zn fractionation on contaminated soils (Couder et al., 2015).
551 However similar water supply and exposition rule out such influence in our setting. The gradient of Cu
552 isotope ratios together with high Cu concentration points towards an immobilization mechanism of Cu in
553 leaves (Blotevogel et al., 2016). The immobilization of Cu as Cu(I)-S groups favors light isotope
554 enrichment in leaves and could thus explain our observations (Collin et al., 2014; Ehrlich et al., 2004;
555 Jouvin et al., 2012; Mathur et al., 2005; Zhu et al., 2002).

556 Finally, small but significant differences in plant nutrition have been detected for various elements
557 including some essential nutrients. It is difficult to directly link these differences to differences in soil
558 chemistry. Yet it has been established that differences in bioavailability in elements can induce different
559 elemental contents in plant tissues (Kuppusamy et al., 2018; Tyler and Olsson, 2001). Note that, these
560 differences do not necessarily include the element whose availability changed. That effect is on one hand
561 due to plant homeostasis mechanisms that can keep tissue concentration especially of essential
562 nutrients constant for a wide range of availability (Marschner and Marschner, 2012); on the other hand
563 regulation mechanisms of plants are not totally independent and exclusive for one element, so that
564 chemically similar elements can be taken up “passively along the way” (Ehlken and Kirchner, 2002; Tyler,
565 2004). However, as factors other than soil chemistry are comparable between the two plots, we
566 attribute detected differences to differences in soil chemistry.

567 In leaves, significant differences between the two plots were detected for the essential nutrients S, K and
568 Zn. Note that higher concentrations were measured in plants grown on the C catena with more
569 calcareous soils. No clear link can be drawn from leaf content to wine properties, still different tissue
570 content of essential nutrients can have an impact on plant biosynthesis (Marschner and Marschner,
571 2012). In grapes, significant differences include concentrations and ratios of K and Ca, elements known

572 for their role in wine acidity and polyphenol synthesis (Brunetto et al., 2015; Daudt and Fogaça, 2008).
573 Potassium was more concentrated in grapes from the C catena whereas Ca was more concentrated in
574 the B catena, highlighting the difference in the ratio between both elements (Table 3), which is
575 particularly important for wine acidity (Brunetto et al., 2015; Daudt and Fogaça, 2008). It is interesting to
576 note that lower Ca concentrations were detected in grapes grown on soils with higher Ca content. This
577 observation highlights the regulation mechanisms carried out by plant during mineral nutrition, and
578 especially during element uptake from soil. But it also puts in evidence the distinct role of sink and
579 source organs (Joubert, 2013) during element translocation from the roots to the different shoots
580 compartments (leaves or grapes). Finally, via the uptake of elements and then their translocation
581 through the plant, this study highlights possible pathways of the influence of soil chemistry on wine
582 properties.

583

584 **Conclusion**

585 In the two examined Soave plots, pedologic differences are obvious from field observations. However,
586 complex formation processes and interlayering of the different bedrocks resulted in rather homogenous
587 chemical composition of soils. This shows that soils that appear to be morphologically different can have
588 similar chemical functioning in terms of element mobility, retention and bioavailability.

589 The pedogenetic processes and the mechanisms involved in mineral nutrition in the Soave vineyard have
590 then been investigated through the elemental contents in the soil-to-grape continuum and the isotope
591 ratios for Cu and Sr. In the Soave vineyard, similar soil chemistry is reflected by similar elemental
592 concentrations in grapevine leaves, although there appears to be a trend for higher elemental
593 concentration in plants grown on more calcareous soil. Moreover, elements are finally not identically
594 distributed in the plants form the two catena and along the different plant tissues (especially leaves or

595 grapes) implying different regulation mechanisms during the soil-to-grape continuum, through uptake
596 and translocation processes. Most importantly K and Ca contents and their ratio, known for regulating
597 wine acidity, vary significantly between the two plots.

598 Isotope ratios measurements show that radiogenic Sr isotopes compositions can be used as a tracer of
599 the geological origin of grapevine nutrition, whereas Cu isotope ratios rather depend on plant regulation
600 mechanisms.

601 Finally, as methods presented in this paper give first indications on the role of soil chemistry in the
602 potential “terroir effect”, it would be possible to go further by improving the sampling strategy (more
603 contrasted soils with a higher number of sampling points, sampling tissues at different vine growth
604 stages, and over several years). However, attention must be given to the other “terroir” components as
605 meteorological parameters, agricultural practices management in the field, winemaking process, etc. in
606 order to more isolate the soil influence.

607

608

609 **Acknowledgments**

610 The authors would like to thank the French INSU national program EC2CO (BIOEFFECT) for its financial
611 help in the TERVIT program. We also want to express our gratitude to Rémi Freydier from AETE-ISO
612 "Analyse des Eléments en Trace dans l’Environnement & ISOtopes" Technical Platform, Philippe Telouk
613 from ENS Lyon and Issam Moussa from the SHIVA platform in Toulouse, for their precious help in
614 elemental contents and isotopes analyses. Finally, we would like to address a very special thanks to
615 Filippo Filippi, the Italian wine grower and winemarker for providing us technical information, allowing
616 us to collect samples in his vineyard and for his kindly and warm welcome in Castelcerino (Soave, Italy).

617 **References**


618 Almeida, C., Vasconcelos, M., 2001. ICP-MS determination of strontium isotope ratio in wine in order to
619 be used as a fingerprint of its regional origin. Journal of analytical atomic spectrometry 16, 607–
620 611. https://doi.org/10.1039/b100307k
621 Almeida, C.M.R., Vasconcelos, M.T.S.D., 2003. Multielement Composition of Wines and Their Precursors
622 Including Provenance Soil and Their Potentialities As Fingerprints of Wine Origin. Journal of
623 Agricultural and Food Chemistry 51, 4788–4798. https://doi.org/10.1021/jf034145b
624 Angel Amoros, J., Perez-de-los Reyes, C., Garcia Navarro, F.J., Bravo, S., Luis Chacon, J., Martinez, J.,
625 Jimenez Ballesta, R., 2013. Bioaccumulation of mineral elements in grapevine varieties cultivated
626 in "La Mancha." JOURNAL OF PLANT NUTRITION AND SOIL SCIENCE 176, 843–850.
627 https://doi.org/10.1002/jpln.201300015
628 Arrouays, D., Saby, N., Thioulouse, J., Jolivet, C., Boulonne, L., Ratié, C., 2011. Large trends in French
629 topsoil characteristics are revealed by spatially constrained multivariate analysis. Geoderma 161,
630 Issues 3–4, 107-114.
631 Babcsányi, I., Chabaux, F., Granet, M., Meite, F., Payraudeau, S., Duplay, J., Imfeld, G., 2016. Copper in
632 soil fractions and runoff in a vineyard catchment: Insights from copper stable isotopes. Science
633 of The Total Environment 557–558, 154–162. https://doi.org/10.1016/j.scitotenv.2016.03.037
634 Babcsányi, I., Imfeld, G., Granet, M., Chabaux, F., 2014. Copper Stable Isotopes To Trace Copper Behavior
635 in Wetland Systems. Environmental Science & Technology 48, 5520–5529.
636 https://doi.org/10.1021/es405688vBao, H., Kao, S.J., Lee, T.Y., Zehetner, F., Huang, J.C., Chang,
637 Y.P., Lu, J.T., Lee, J.Y., 2017. Distribution of organic carbon and lignin in soils in a subtropical
638 small mountainous river basin. Geoderma 306, 81-88.
639 Bassi, D., Nebelsick, J.H., 2010. Components, facies and ramps: Redefining Upper Oligocene shallow
640 water carbonates using coralline red algae and larger foraminifera (Venetian area, northeast
641 Italy). PALAEOGEOGRAPHY PALAEOCLIMATOLOGY PALAEOECOLOGY 295, 258–280.
642 https://doi.org/10.1016/j.palaeo.2010.06.003
643 Benciolini, G., Tomasi, D., Pascarella, G., Lorenzoni, A., Verze, G., 2006. Soave Viticultural zoning: the soil
644 as affecting wine quality. BOLLETTINO DELLA SOCIETA GEOLOGICA ITALIANA 135–146.
645 Bertoldi, D., Larcher, R., Bertamini, M., Otto, S., Concheri, G., Nicolini, G., 2011. Accumulation and
646 Distribution Pattern of Macro- and Microelements and Trace Elements in Vitis vinifera L. cv.
647 Chardonnay Berries. Journal of Agricultural and Food Chemistry 59, 7224–7236.
648 https://doi.org/10.1021/jf2006003
649 Bigalke, M., Weyer, S., Wilcke, W., 2010. Stable Copper Isotopes: A Novel Tool to Trace Copper Behavior
650 in Hydromorphic Soils. Soil Science Society of America Journal 74, 60.
651 https://doi.org/10.2136/sssaj2008.0377
652 Blotevogel, S., Oliva, P., Sobanska, S., Viers, J., Vezin, H., Audry, S., Prunier, J., Darrozes, J., Orgogozo, L.,
653 Courjault-Radé, P., Schreck, E., 2018. The fate of Cu pesticides in vineyard soils: A case study
654 using δ 65 Cu isotope ratios and EPR analysis. Chemical Geology 477, 35–46.
655 https://doi.org/10.1016/j.chemgeo.2017.11.032
656 Blum, J., Taliaferro, E., Weisse, M., Holmes, R., 2000. Changes in Sr/Ca, Ba/Ca and Sr-87/Sr-86 ratios
657 between trophic levels in two forest ecosystems in the northeastern USA. BIOGEOCHEMISTRY
658 49, 87–101. https://doi.org/10.1023/A:1006390707989
659 Boselli, M., Vaio, C.D., Pica, B., 1998. Effect of soil moisture and transpiration on mineral content in
660 leaves and berries of cabernet sauvignon grapevine. Journal of Plant Nutrition 21, 1163–1178.
661 https://doi.org/10.1080/01904169809365475

662 Bramley, R.G.V., Ouzman, J., Boss, P.K., 2011. Variation in vine vigour, grape yield and vineyard soils and
663 topography as indicators of variation in the chemical composition of grapes, wine and wine
664 sensory attributes. AUSTRALIAN JOURNAL OF GRAPE AND WINE RESEARCH 17, 217–229.
665 https://doi.org/10.1111/j.1755-0238.2011.00136.xBraschi, E., Marchionni, S., Priori, S., Casalini,
666 M., Tommasini, S., Natarelli, L., Buccianti, A., Bucelli, P., Costantini, E.A.C., Conticelli, S., 2018.
667 Tracing the 87 Sr/ 86 Sr from rocks and soils to vine and wine: An experimental study on geologic
668 and pedologic characterisation of vineyards using radiogenic isotope of heavy elements. Science
669 of The Total Environment 628–629, 1317–1327. https://doi.org/10.1016/j.scitotenv.2018.02.069
670
671 Brunetto, G., Bastos De Melo, G.W., Toselli, M., Quartieri, M., Tagliavini, M., 2015. THE ROLE OF
672 MINERAL NUTRITION ON YIELDS AND FRUIT QUALITY IN GRAPEVINE, PEAR AND APPLE. REVISTA
673 BRASILEIRA DE FRUTICULTURA 37, 1089–1104. https://doi.org/10.1590/0100-2945-103/15
674 Caldelas, C., Weiss, D.J., 2017. Zinc Homeostasis and isotopic fractionation in plants: a review. Plant and
675 Soil 411, 17–46. https://doi.org/10.1007/s11104-016-3146-0
676 Capo, R., Stewart, B., Chadwick, O., 1998. Strontium isotopes as tracers of ecosystem processes: theory
677 and methods. GEODERMA 82, 197–225. https://doi.org/10.1016/S0016-7061(97)00102-X
678 Castro, P.H., Lilay, G.H., Assunção, A.G.L., 2018. Chapter 1 - Regulation of Micronutrient Homeostasis and
679 Deficiency Response in Plants. In: Plant Micronutrient Use Efficiency, Academic Press, 2018,
680 Pages 1-15.
681 Ciesielski, H., Sterckeman, T., 1997. A comparison between three methods for the determination of
682 cation exchange capacity and exchangeable cations in soils. Agronomie, 17, 9-15.
683 Chopin, E.I.B., Marin, B., Mkoungafoko, R., Rigaux, A., Hopgood, M.J., Delannoy, E., Canès, B., Laurain,
684 M., 2008. Factors affecting distribution and mobility of trace elements (Cu, Pb, Zn) in a perennial
685 grapevine (Vitis vinifera, L.) in the champagne region of France. Environ. Pollut. 156, 1092-1098.
686 Coetzee, P.P., van Jaarsveld, F.P., Vanhaecke, F., 2014. Intraregional classification of wine via ICP-MS
687 elemental fingerprinting. Food Chemistry 164, 485–492.
688 https://doi.org/10.1016/j.foodchem.2014.05.027Collin, B., Doelsch, E., Keller, C., Cazevieille, P.,
689 Tellac, M., Chaurand, P., Panfili, F., Hazemann, J.L., Meunier, J.D., 2014. Evidence of sulfur-bound
690 reduced copper in bamboo exposed to high silicon and copper concentrations. Environmental
691 Pollution 187, 22-30.
692 Couder, E., Mattielli, N., Drouet, T., Smolders, E., Delvaux, B., Iserentant, A., Meeus, C., Maerschalk, C.,
693 Opfergelt, S., Houben, D., 2015. Transpiration flow controls Zn transport in Brassica napus and
694 Lolium multiflorum under toxic levels as evidenced from isotopic fractionation. Comptes Rendus
695 Geoscience 347, 386–396. https://doi.org/10.1016/j.crte.2015.05.004
696 Cugnetto, A., Santagostini, L., Rolle, L., Guidoni, S., Gerbi, V., Novello, V., 2014. Tracing the “terroirs” via
697 the elemental composition of leaves, grapes and derived wines in cv Nebbiolo (Vitis vinifera L.).
698 Scientia Horticulturae 172, 101–108. https://doi.org/10.1016/j.scienta.2014.03.055
699 Daudt, C.E., Fogaça, A. de O., 2008. Efeito do ácido tartárico nos valores de potássio, acidez titulável e pH
700 durante a vinificação de uvas Cabernet Sauvignon. Ciência Rural 38, 2345–2350.
701 https://doi.org/10.1590/S0103-84782008000800039
702 Day, M.P., Zhang, B., Martin, G.J., 1995. Determination of the geographical origin of wine using joint
703 analysis of elemental and isotopic composition. II—Differentiation of the principal production
704 zones in france for the 1990 vintage. Journal of the Science of Food and Agriculture 67, 113–123.
705 https://doi.org/10.1002/jsfa.2740670118
706 De Vecchi, G., Gregnanin, A., Piccirillo, E.M., 1976. Tertiary volcanism in the veneto: Magmatology,
707 petrogenesis and geodynamic implications. Geologische Rundschau 65, 701–710.
708 https://doi.org/10.1007/BF01808487

709 Durante, C., Baschieri, C., Bertacchini, L., Bertelli, D., Cocchi, M., Marchetti, A., Manzini, D., Papotti, G.,
710 Sighinolfi, S., 2015. An analytical approach to Sr isotope ratio determination in Lambrusco wines
711 for geographical traceability purposes. Food Chemistry 173, 557–563.
712 https://doi.org/10.1016/j.foodchem.2014.10.086
713 Durante, C., Baschieri, C., Bertacchini, L., Cocchi, M., Sighinolfi, S., Silvestri, M., Marchetti, A., 2013.
714 Geographical traceability based on 87Sr/86Sr indicator: A first approach for PDO Lambrusco
715 wines from Modena. Food Chemistry 141, 2779–2787.
716 https://doi.org/10.1016/j.foodchem.2013.05.108
717 Durante, C., Bertacchini, L., Cocchi, M., Manzini, D., Marchetti, A., Rossi, M.C., Sighinolfi, S., Tassi, L.,
718 2018. Development of 87 Sr/ 86 Sr maps as targeted strategy to support wine quality. Food
719 Chemistry 255, 139–146. https://doi.org/10.1016/j.foodchem.2018.02.084
720 Ehlken, S., Kirchner, G., 2002. Environmental processes affecting plant root uptake of radioactive trace
721 elements and variability of transfer factor data: a review. Journal of Environmental Radioactivity
722 58, 97–112. https://doi.org/10.1016/S0265-931X(01)00060-1Ehrlich, S., Butler, I., Halicz Richard,
723 D., Oldroyd, A., Matthews A., 2004. Experimental study of the copper fractionation between
724 aqueous (CuII) and colellite (CuS). Chemical Geology 209, 259-269.
725 Epke, E.M., Lawless, H.T., 2007. Retronasal smell and detection thresholds of iron and copper salts.
726 PHYSIOLOGY & BEHAVIOR 92, 487–491.
727 https://doi.org/10.1016/j.physbeh.2007.04.022FAO/ISRIC/ISSS, 1998. World reference base for
728 soil resources International soil classification system for naming soils and creating legends for
729 soil maps. World Soil Resources Reports 84, 1–87. Update 2015, Rome.
730 Farquhar, G.D., Ehleringer, J.R., Hubick, K.T., 1989. Carbon Isotope Discrimination and Photosynthesis.
731 Annual Review of Plant Physiology and Plant Molecular Biology 40, 503–537.
732 https://doi.org/10.1146/annurev.pp.40.060189.002443
733 Fekiacova, Z., Cornu, S., Pichat, S., 2015. Tracing contamination sources in soils with Cu and Zn isotopic
734 ratios. Science of The Total Environment 517, 96–105.
735 https://doi.org/10.1016/j.scitotenv.2015.02.046
736 Gómez-Alonso, S., García-Romero, E., 2009. Effect of irrigation and variety on oxygen (δ18O) and carbon
737 (δ13C) stable isotope composition of grapes cultivated in a warm climate: Irrigation, variety and
738 grape δ18O and δ13C values. Australian Journal of Grape and Wine Research 16, 283–289.
739 https://doi.org/10.1111/j.1755-0238.2009.00089.x
740 Gonzalez-Barreiro, C., Rial-Otero, R., Cancho-Grande, B., Simal-Gandara, J., 2015. Wine Aroma
741 Compounds in Grapes: A Critical Review. CRITICAL REVIEWS IN FOOD SCIENCE AND NUTRITION 55, 202–
742 218. https://doi.org/10.1080/10408398.2011.650336
743 Grechi, I., Vivin, P., Hilbert, G., Milin, S., Robert, T., Gaudillère, J.-P., 2007. Effect of light and nitrogen
744 supply on internal C:N balance and control of root-to-shoot biomass allocation in grapevine.
745 Environmental and Experimental Botany 59, 139–149.
746 https://doi.org/10.1016/j.envexpbot.2005.11.002
747 Greenough, J.D., Mallory-Greenough, L.M., Fryer, B.J., 2005. Geology and wine 9: Regional trace element
748 fingerprinting of Canadian wines. GEOSCIENCE CANADA 32, 129–137.
749 HORN, P., SCHAAF, P., HOLBACH, B., HOLZL, S., ESCHNAUER, H., 1993. SR-87/SR-86 FROM ROCK AND
750 SOIL INTO VINE AND WINE. ZEITSCHRIFT FUR LEBENSMITTEL-UNTERSUCHUNG UND-FORSCHUNG
751 196, 407–409. https://doi.org/10.1007/BF01190802
752 Jobbagy, E., Jackson, R., 2001. The distribution of soil nutrients with depth: Global patterns and the
753 imprint of plants. BIOGEOCHEMISTRY 53, 51–77. https://doi.org/10.1023/A:1010760720215
754 Joubert, C., 2013. A case study of source-sink relationships using shoot girdling and berry classification
755 (Vitis vinifera cv. Cabernet Sauvignon). Masters thesis, Stellenbosch University.

Jouvin, D., Weiss, D.J., Mason, T.F.M., Bravin, M.N., Louvat, P., Zhao, F., Ferec, F., Hinsinger, P., Benedetti, M.F., 2012. Stable Isotopes of Cu and Zn in Higher Plants: Evidence for Cu Reduction at the Root Surface and Two Conceptual Models for Isotopic Fractionation Processes. Environmental Science & Technology 46, 2652–2660. https://doi.org/10.1021/es202587m

Kabata-Pendias, A., 2004. Soil–plant transfer of trace elements—an environmental issue. Geoderma 122, 143–149. http://dx.doi.org/10.1016/j.geoderma.2004.01.004Kania, M., Gautier, M., Imig, A., Michel, P., Gourdon, R., 2019. Comparative characterization of surface sludge deposits from fourteen French Vertical Flow Constructed Wetlands sewage treatment plants using biological, chemical and thermal indices. Science of The Total Environment 647, 464-473.

Ko, B.G., Vogeler, I., Bolan, N.S., Clothier, B., Green, S., Kennedy, J., 2007. Mobility of copper, chromium and arsenic from treated timber into grapevines. Science of the Total Environment 388, 35-42.

Kuhnholtz-Lordat, G., 1963. La genèse des appellations d'origine des vins. Imprimerie Buguet-Comptour, Macon.

Kuppusamy, S., Yoon, Y.-E., Kim, S.Y., Kim, J.H., Kim, H.T., Lee, Y.B., 2018. Does long-term application of fertilizers enhance the micronutrient density in soil and crop?—Evidence from a field trial conducted on a 47-year-old rice paddy. Journal of Soils and Sediments 18, 49–62. https://doi.org/10.1007/s11368-017-1743-z

Kwan, W.-O., Kowalski, B.R., Skogerboe, R.K., 1979. Pattern recognition analysis of elemental data. Wines of Vitis vinifera cv Pinot Noir from France and the United States. Journal of Agricultural and Food Chemistry 27, 1321–1326. https://doi.org/10.1021/jf60226a039

Langmuir, C.H., Vocke, R.D., Hanson, G.N., Hart, S.R., 1978. A general mixing equation with applications to Icelandic basalts. Earth and Planetary Science Letters 37, 380–392. https://doi.org/10.1016/0012-821X(78)90053-5

Li, S.-Z., Zhu, X.-K., Wu, L.-H., Luo, Y.-M., 2016. Cu isotopic compositions in Elsholtzia splendens: Influence of soil condition and growth period on Cu isotopic fractionation in plant tissue. Chemical Geology 444, 49–58. https://doi.org/10.1016/j.chemgeo.2016.09.036

Likar, M., Vogel-Mikus, K., Potisek, M., Hancevic, K., Radic, T., Necemer, M., Regvar, M., 2015. Importance of soil and vineyard management in the determination of grapevine mineral composition. SCIENCE OF THE TOTAL ENVIRONMENT 505, 724–731. https://doi.org/10.1016/j.scitotenv.2014.10.057

Mackenzie, D., Christy, A., 2005. The role of soil chemistry in wine grape quality and sustainable soil management in vineyards. Water Science and Technology 51, 27–37.

Maltman, A., 2013. Minerality in wine: a geological perspective. Journal of Wine Research 24, 169–181. https://doi.org/10.1080/09571264.2013.793176

Maltman, A., 2008. The Role of Vineyard Geology in Wine Typicity. Journal of Wine Research 19, 1–17. https://doi.org/10.1080/09571260802163998

Maréchal, C.N., Télouk, P., Albarède, F., 1999. Precise analysis of copper and zinc isotopic compositions by plasma-source mass spectrometry. Chemical Geology 156, 251–273. https://doi.org/10.1016/S0009-2541(98)00191-0Marchionni, S., Braschi, E., Tommasini, S., Bollati, A., Cifelli, F., Mulinacci, N., Mattei, M., Conticelli, S., 2013. High-Precision 87Sr/86Sr Analyses in Wines and Their Use as a Geological Fingerprint for Tracing Geographic Provenance. Journal of Agricultural and Food Chemistry 61, 6822–6831. https://doi.org/10.1021/jf4012592

Marchionni, S., Buccianti, A., Bollati, A., Braschi, E., Cifelli, F., Molin, P., Parotto, M., Mattei, M., Tommasini, S., Conticelli, S., 2016. Conservation of 87 Sr/ 86 Sr isotopic ratios during the winemaking processes of 'Red' wines to validate their use as geographic tracer. Food Chemistry 190, 777–785. https://doi.org/10.1016/j.foodchem.2015.06.026

Marschner, H., Marschner, P. (Eds.), 2012. Marschner's Mineral nutrition of higher plants, 3. ed. ed. Elsevier, Academic Press, Amsterdam.Martins, P., Madeira, M., Monteiro, F., Bruno de Sousa, R.,

804 Curvelo-Garcia, A., Catarino, S., 2014. 7Sr/86Sr ratio in vineyard soils from Portuguese
805 denominations of origin and its potential for origin authentication. J. Int. Sci. Vigne Vin 48, n°1,
806 21-29.
807 Mathur, R., Ruiz, J., Titley, S., Liermann, L., Buss, H., Brantley, S., 2005. Cu isotopic fractionation in the
808 supergene environment with and without bacteria. Geochimica and Cosmochimica Acta 69, Issue
809 22, 5233-5246.
810 Mercurio, M., Grilli, E., Odierna, P., Morra, V., Prohaska, T., Coppola, E., Grifa, C., Buondonno, A.,
811 Langella, A., 2014. A 'Geo-Pedo-Fingerprint' (GPF) as a tracer to detect univocal parent material-
812 to-wine production chain in high quality vineyard districts, Campi Flegrei (Southern Italy).
813 Geoderma 230–231, 64–78. http://dx.doi.org/10.1016/j.geoderma.2014.04.006
814 Mihaljevič, M., Jarošíková, A., Ettler, V., Vaněk, A., Penížek, V., Kříbek, B., Chrastný, V., Sracek, O., Trubač,
815 J., Svoboda, M., Nyambe, I., 2018. Copper isotopic record in soils and tree rings near a copper
816 smelter, Copperbelt, Zambia. Science of The Total Environment 621, 9–17.
817 https://doi.org/10.1016/j.scitotenv.2017.11.114
818 Munsell, A., 2000. Munsell Soil Color Charts. Revised Edition Gretag Macbeth, New Windsor, New York
819 (update 2000 from 1994 first version).Orsini, L., Remy J.C., 1976. Utilisation du chlorure de
820 cobaltihexammine pour la détermination simultanée de la capacité d'échange et des bases
821 échangeables des sols. Sci. Sol 4, 269-275.
822 Pereira, C.F., 1988. The importance of metallic elements in wine. A literature survey. Zeitschrift für
823 Lebensmittel-Untersuchung und Forschung 186, 295–300.
824 https://doi.org/10.1007/BF01027030Petrini, R., Sansone, L., Slejko, F.F., Buccianti, A., Marcuzzo,
825 P., Tomasi, D., 2015. The 87Sr/86Sr strontium isotopic systematics applied to Glera vineyards: A
826 tracer for the geographical origin of the Prosecco. Food Chemistry 170, 138–144.
827 https://doi.org/10.1016/j.foodchem.2014.08.051
828 Peuke, A., 2000. The chemical composition of xylem sap in Vitis vinifera L. cv. riesling during vegetative
829 growth on three different franconian vineyard soils and as influenced by nitrogen fertilizer.
830 AMERICAN JOURNAL OF ENOLOGY AND VITICULTURE 51, 329–339.
831 Pohl, P., 2007. What do metals tell us about wine? TrAC Trends in Analytical Chemistry 26, 941–949.
832 http://dx.doi.org/10.1016/j.trac.2007.07.005
833 Porchet, M., Laferre, H., 1935. Détermination des caractéristiques hydro-dynamiques des sols en place.
834 Mémoire et notes techniques. Annales du Ministèere de l'Agriculture 568.
835 Poszwa, A., Dambrine, E., Pollier, B., Atteia, O., 2000. A comparison between Ca and Sr cycling in forest
836 ecosystems. PLANT AND SOIL 225, 299–310. https://doi.org/10.1023/A:1026570812307
837 Ramos, M.C., 2017. Projection of phenology response to climate change in rainfed vineyards in north-
838 east Spain. Agricultural and Forest Meteorology 247, 104–115.
839 https://doi.org/10.1016/j.agrformet.2017.07.022
840 Ramos, M.C., Martínez-Casasnovas, J.A., 2006. Impact of land levelling on soil moisture and runoff
841 variability in vineyards under different rainfall distributions in a Mediterranean climate and its
842 influence on crop productivity. Journal of Hydrology 321, 131–146.
843 https://doi.org/10.1016/j.jhydrol.2005.07.055
844 Rietra, R.P.J.J., Heinen, M., Dimkpa, C.O., Bindraban, P.S., 2017. Effects of Nutrient Antagonism and
845 Synergism on Yield and Fertilizer Use Efficiency. Communications in Soil Science and Plant
846 Analysis 48(16), 1895-1920.
847 Ryan, B.M., Kirby, J.K., Degryse, F., Harris, H., McLaughlin, M.J., Scheiderich, K., 2013. Copper speciation
848 and isotopic fractionation in plants: uptake and translocation mechanisms. New Phytologist 199,
849 367–378. https://doi.org/10.1111/nph.12276

Scherz, H., Kirchhoff, E., 2006. Trace elements in foods: Zinc contents of raw foods—A comparison of data originating from different geographical regions of the world. Journal of Food Composition and Analysis 19, 420–433. https://doi.org/10.1016/j.jfca.2005.10.004

Schmitt, A.-D., Gangloff, S., Labolle, F., Chabaux, F., Stille, P., 2017. Calcium biogeochemical cycle at the beech tree-soil solution interface from the Strengbach CZO (NE France): insights from stable Ca and radiogenic Sr isotopes. GEOCHIMICA ET COSMOCHIMICA ACTA 213, 91–109. https://doi.org/10.1016/j.gca.2017.06.039

Sipos, L., Kovács, Z., Sági-Kiss, V., Csiki, T., Kókai, Z., Fekete, A., Héberger, K., 2012. Discrimination of mineral waters by electronic tongue, sensory evaluation and chemical analysis. Food Chemistry 135, 2947–2953. https://doi.org/10.1016/j.foodchem.2012.06.021

Strom, L., 1997. Root exudation of organic acids: importance to nutrient availability and the calcifuge and calcicole behaviour of plants. OIKOS 80, 459–466. https://doi.org/10.2307/3546618

Styger, G., Prior, B., Bauer, F.F., 2011. Wine flavor and aroma. Journal of Industrial Microbiology & Biotechnology 38, 1145–1159. https://doi.org/10.1007/s10295-011-1018-4

Tescione, I., Marchionni, S., Casalini, M., Vignozzi, N., Mattei, M., Conticelli, S., 2018. 87 Sr/ 86 Sr isotopes in grapes of different cultivars: A geochemical tool for geographic traceability of agriculture products. Food Chemistry 258, 374–380. https://doi.org/10.1016/j.foodchem.2018.03.083

Tournebize, J., Gregoire, C., Coupe, R.H., Ackerer, P., 2012. Modelling nitrate transport under row intercropping system: Vines and grass cover. Journal of Hydrology 440–441, 14–25. https://doi.org/10.1016/j.jhydrol.2012.03.002

Tyler, G., 2004. Ionic charge, radius, and potential control root/soil concentration ratios of fifty cationic elements in the organic horizon of a beech (Fagus sylvatica) forest podzol. Science of The Total Environment 329, 231–239. https://doi.org/10.1016/j.scitotenv.2004.03.004

Tyler, G., Olsson, T., 2001. Plant uptake of major and minor mineral elements as influenced by soil acidity and liming. PLANT AND SOIL 230, 307–321. https://doi.org/10.1023/A:1010314400976

van Leeuwen, C., TREGOAT, O., CHONÉ, X., BOIS, B., PERNET, D., GAUDILLÈRE, J.-P., 2009. Vine water status is a key factor in grape ripening and vintagequalityfor red Bordeaux wine. How cen it be assessed for vineyard management purposes? J. Int. Sci. Vigne Vin 43, 121–134.

Vaudour, E., Costantini, E., Jones, G.V., Mocali, S., 2015. An overview of the recent approaches to terroir functional modelling, footprinting and zoning. SOIL 1, 287–312. https://doi.org/10.5194/soil-1-287-2015

Vazquez Vazquez, F.A., Perez Cid, B., Segade, S.R., 2016. Assessment of metal bioavailability in the vineyard soil-grapevine system using different extraction methods. FOOD CHEMISTRY 208, 199–208. https://doi.org/10.1016/j.foodchem.2016.04.005Walsh, T., 1945. The Effect on Plant Growth of Substituting Strontium for Calcium in Acid Soils. Proceedings of the Royal Irish Academy. Section B: Biological, Geological, and Chemical Science Vol. 50, 287-294.

Wanogho, S., Gettinby, G., Caddy B., 1987. Particle size distribution analysis of soils using laser diffraction. Forensic Science International 33, Issue 2, 117-128.

Weinstein, C., Moynier, F., Wang, K., Paniello, R., Foriel, J., Catalano, J., Pichat, S., 2011. Isotopic fractionation of Cu in plants. Chemical Geology. https://doi.org/10.1016/j.chemgeo.2011.05.010

Zhu, X.K., Guo, Y., Williams, R.J.P., O'Nions, R.K., Matthews, A., Belshaw, N.S., Canters, G.W., deWaal, E.C.,Weser, U., Burgess, B.K., Salvato, B., 2002. Mass fractionation processes of transition metal isotopes. Earth and Planetary Science Letters 200, 47–62.

## Figures

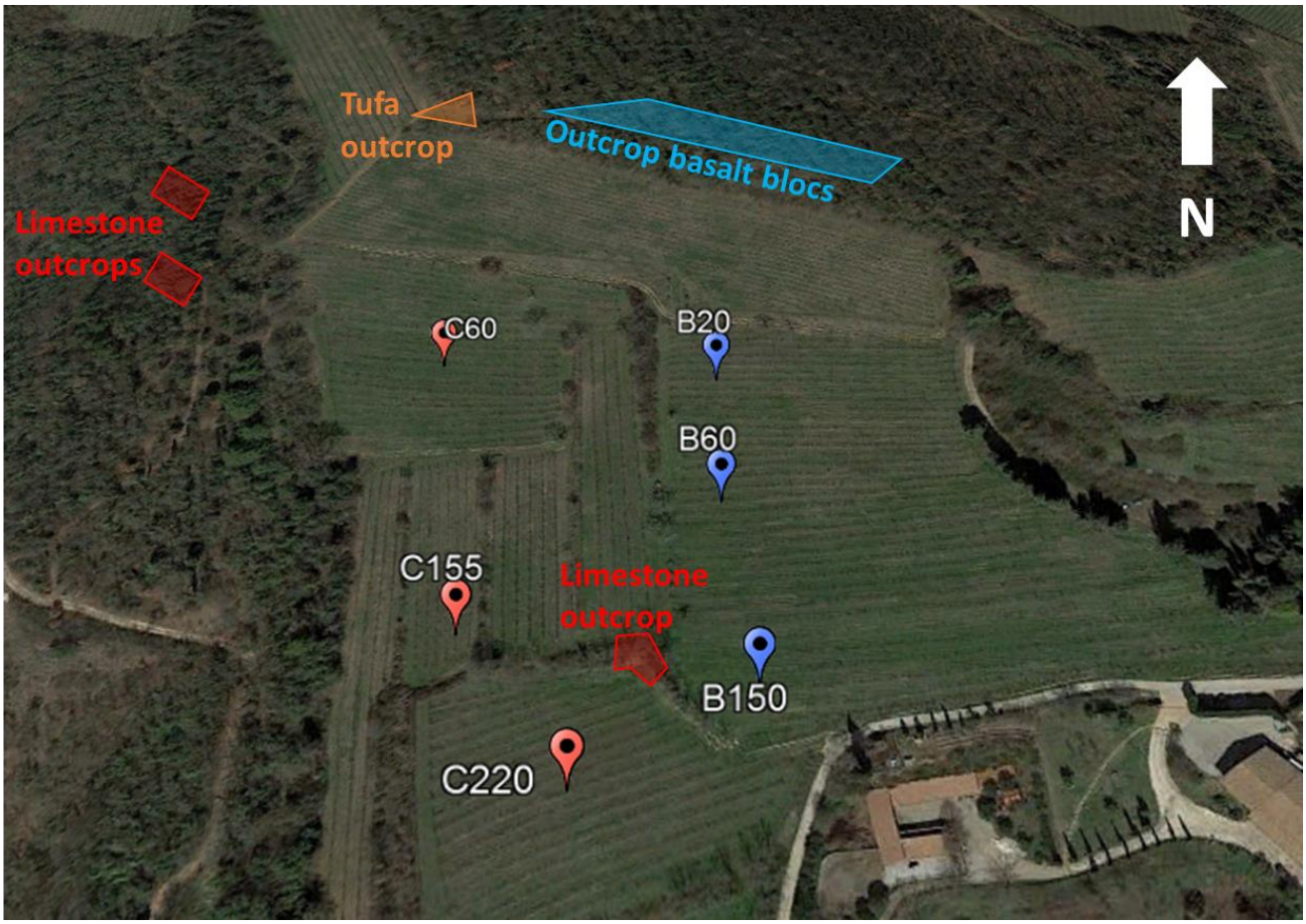


**Figure 1 –** The experimental site in the Soave vineyard including the two catenas. C stands for calcareous (point C60 to C220) and B for basaltic (point B20 to B150). Rock outcrops (basalt, limestone and tufa rocks) are represented by colored areas. The aerial image is taken from Google Earth®.

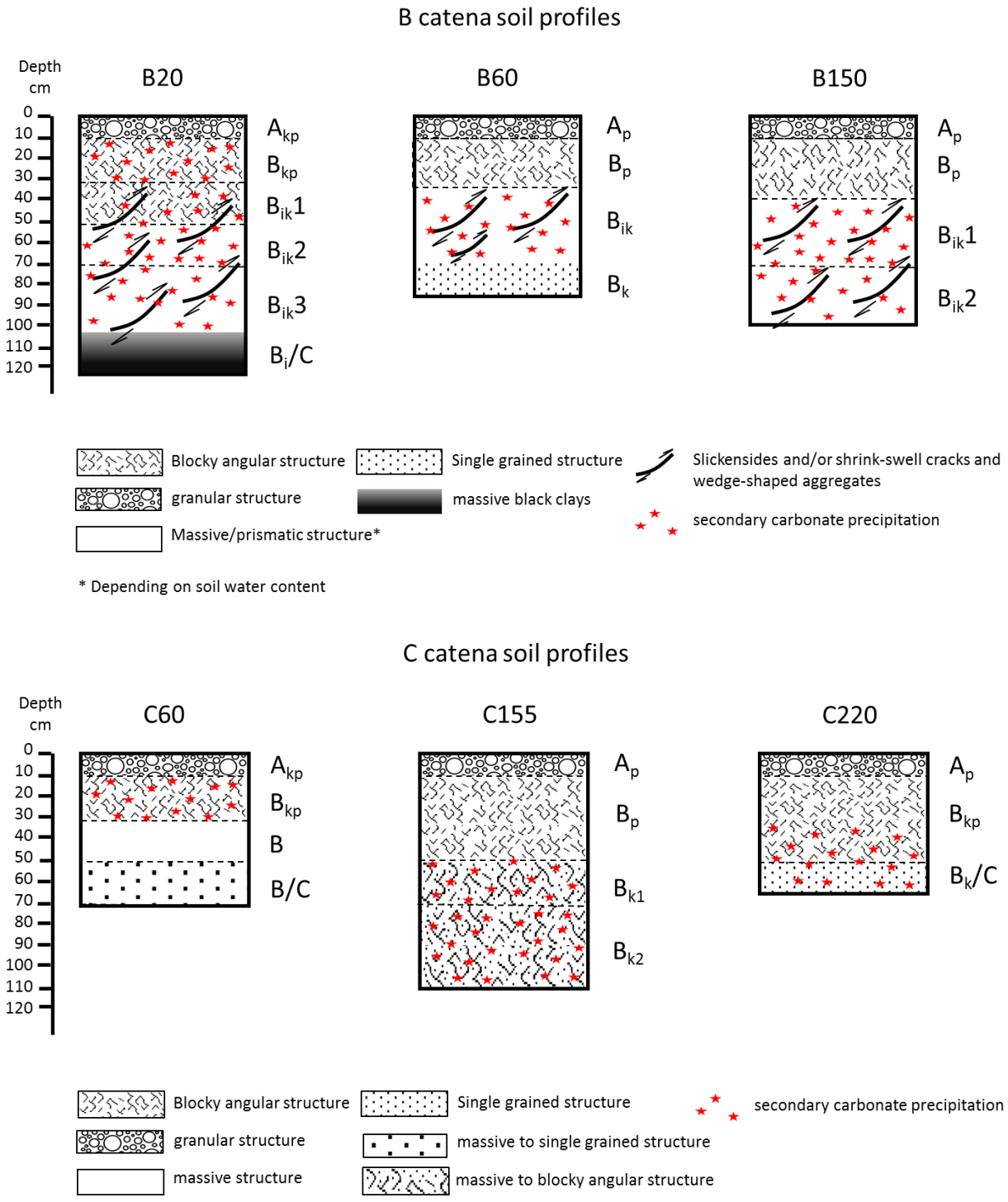


**Figure 2 –** Schematic illustration of the field observations for the soils of the two catenas investigated in the present study (B & C). Roots are particularly thick in the first 10-20 cm for all the sampling points. Soil profile description was stopped according to the soil depth, using an Edelman soil corer down to the depth of 120 cm maximum. Soil structures above 50 cm are indicative structures as structure observation is biased during soil corer sampling.

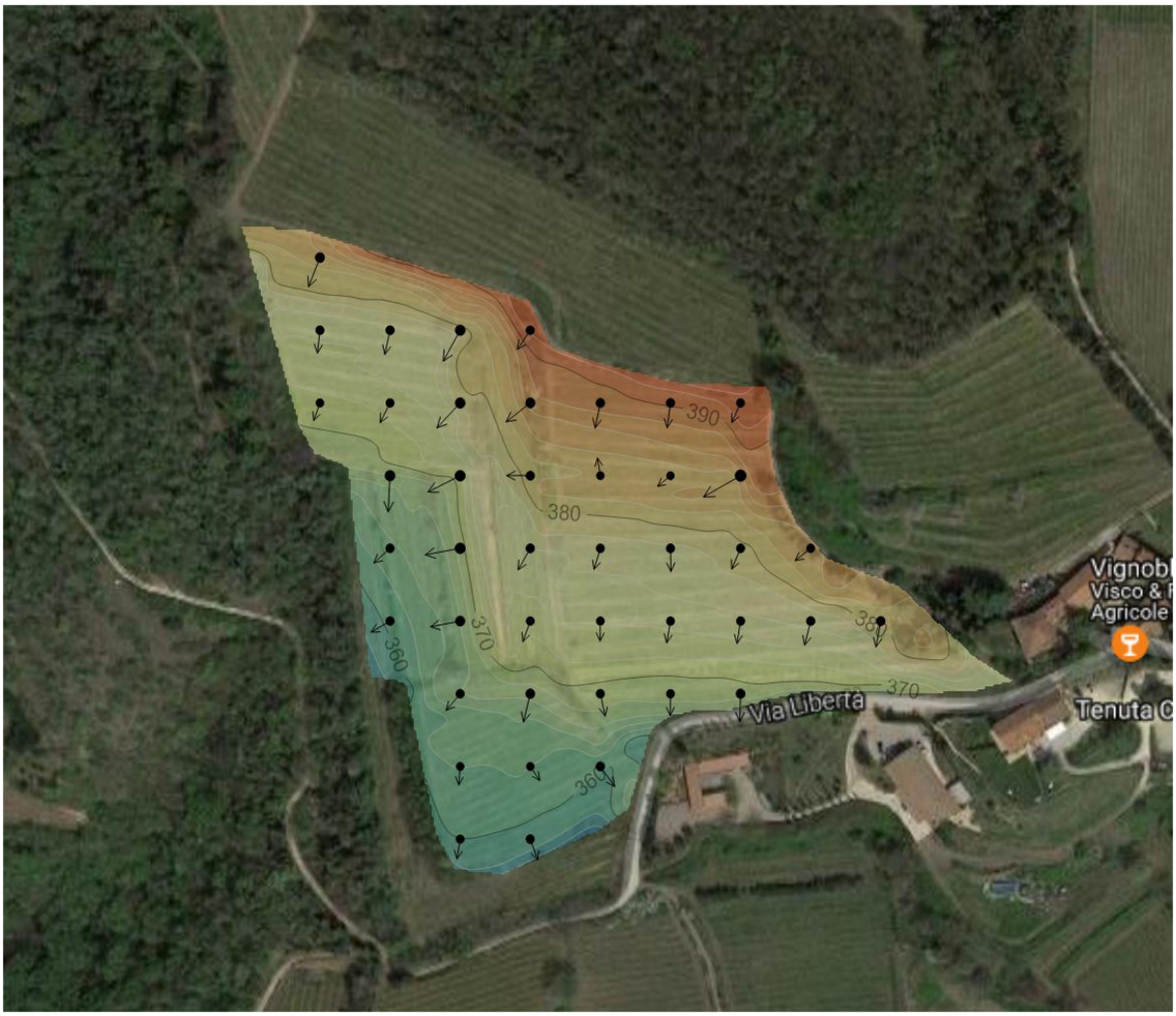


**Figure 3 –** Elevation and slope direction map of the studied vineyard plots. The aerial image is taken from Google Earth®.

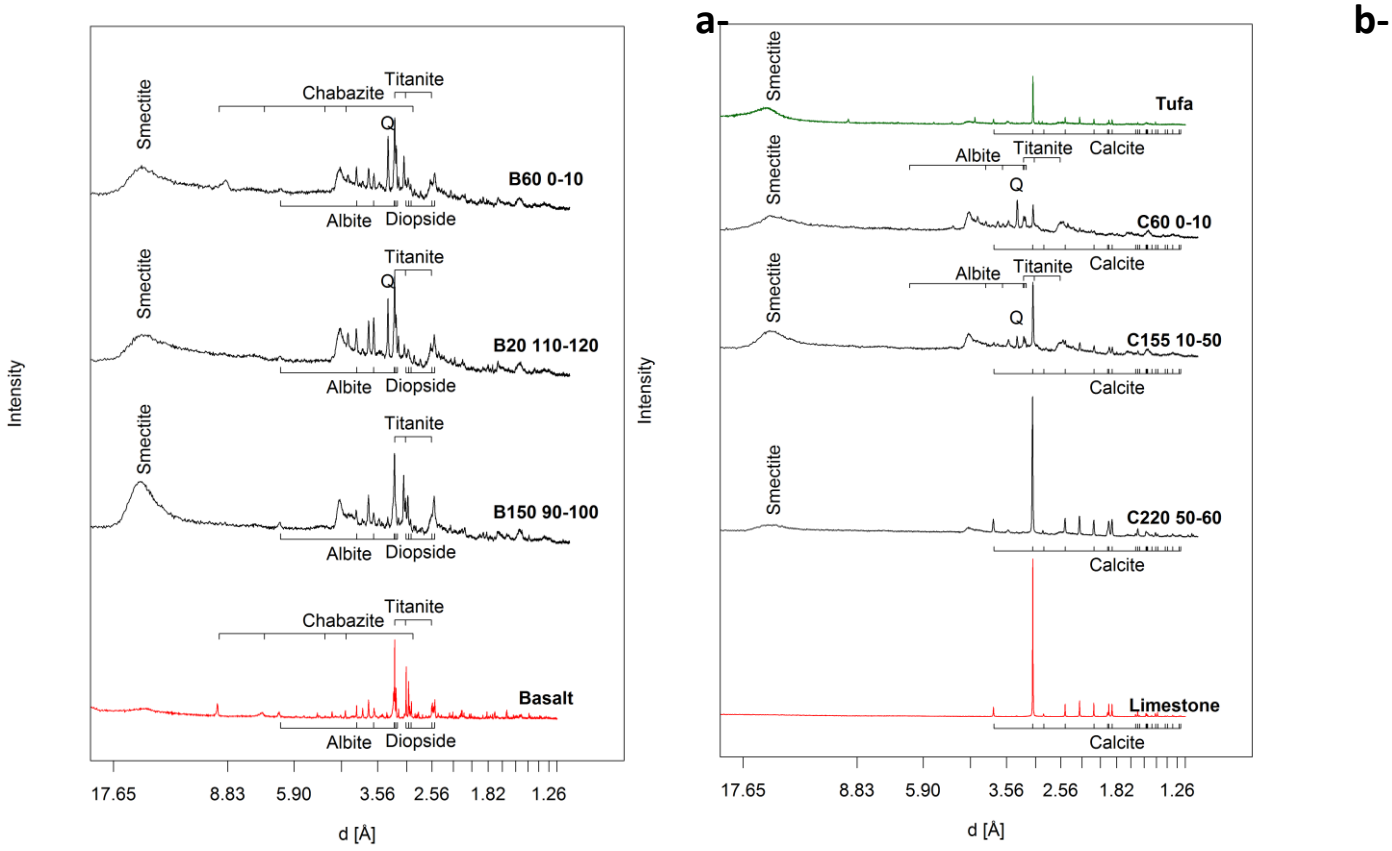


**Figure 4 –** XRD spectra of rocks and soil horizons (a- Basalt rock and B catena; b-Calcareous rock and C catena). For clarity, only the main peaks of the identified phases are reported for silicates (a).

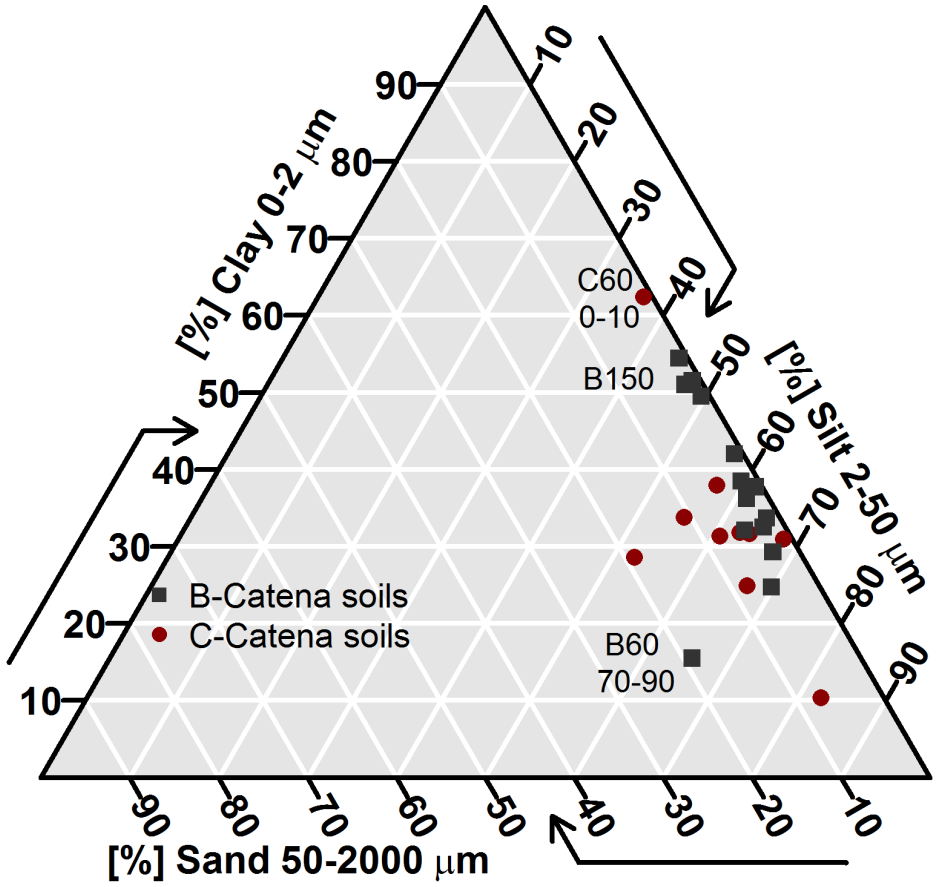


**Figure 5**- Textural triangle of the studied soils after acid treatment to eliminate carbonates.

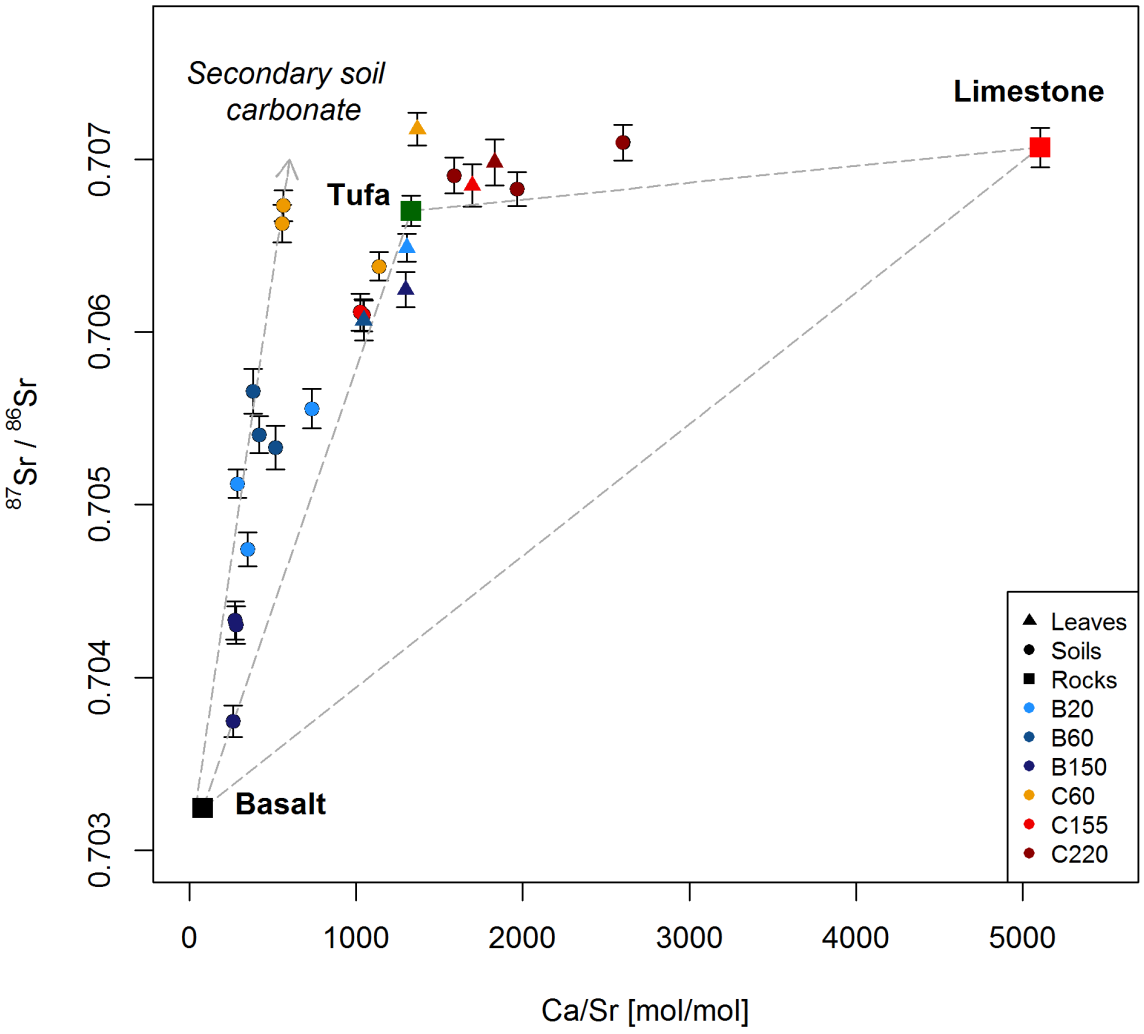


**Figure 6**- Mixing diagram of different source rocks, soils and vine leaves. The arrow on the left represents a hypothetic secondary soil carbonate pool.

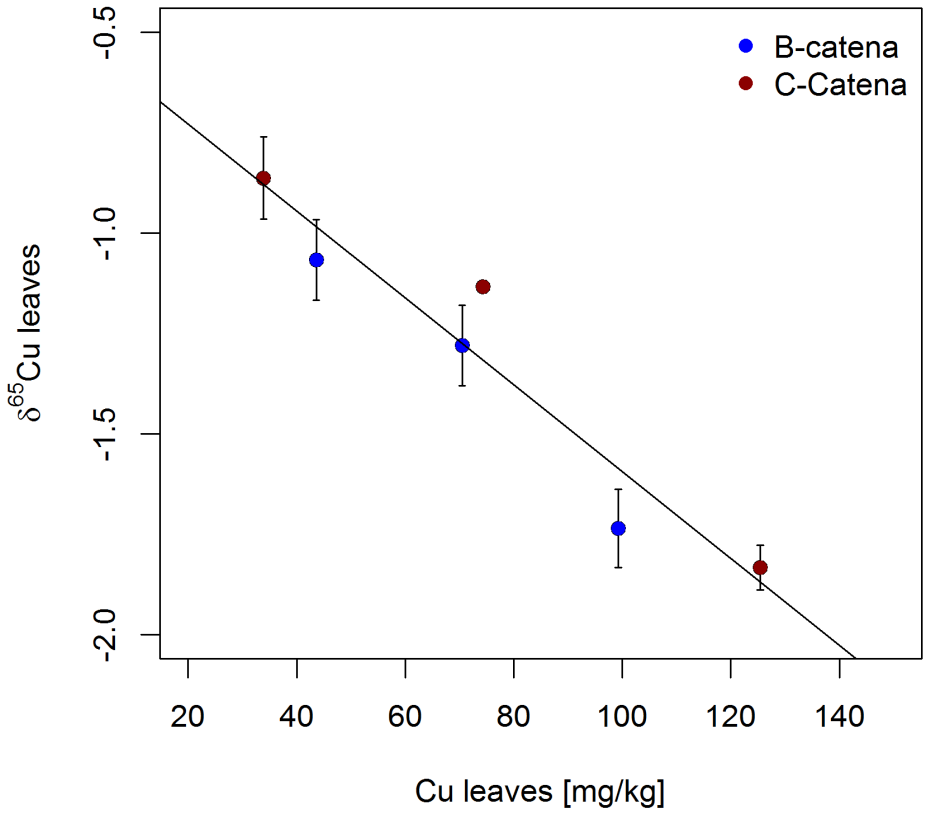


**Figure 7 –** Cu isotope ratios in vine leaves as a function of their Cu-content.

**Table 1-** Mineralogical and physico-chemical properties of Soave soils

| Soil ID and depths (cm) | Horizon (WRB classification) | Mineralogical phases | pH ($H_20$) | CEC | SIC | SOC | Clay | Silt | Sand | K |
|---|---|---|---|---|---|---|---|---|---|---|
| | | | | cmol/kg | wt % | wt % | wt % | wt % | wt % | $m.s^{-1}$ |
| **B20** | | | | | | | | | | $1*10^{-5}$ |
| 0-10 | Mollic, calcic | **calc.**, felds., smec. | 7.51 | 72.12 | 1.8 | 4.3 | 30 | 67 | 3 | |
| 10-30 | Calcic | **calc.**, felds., smec. | 7.67 | 66.13 | 2.2 | 1.3 | 39 | 59 | 2 | |
| 50-70 | Vertic | **felds.**, smec. | 7.80 | 71.91 | 0.5 | 0.7 | 25 | 70 | 5 | |
| 70-120 | Vertic | **felds.**, smec. | 7.74 | 75.23 | <0.1 | 0.8 | 34 | 64 | 2 | |
| **B60** | | | | | | | | | | $2*10^{-6}$ |
| 0-10 | Mollic | **felds.**, smec. | 7.17 | 82.94 | 0.5 | 7.1 | 38 | 61 | 1 | |
| 10-30 | Cambic | **felds.**, smec. | 7.90 | NA | 0.4 | 1.3 | 42 | 57 | 1 | |
| 30-60 | Vertic | **felds.**, smec. | 7.83 | 77.72 | 0.3 | 0.9 | 33 | 66 | 1 | |
| 60-70 | Vertic | **qtz.**, felds., smec. | 7.82 | 78.31 | 0.3 | 0.6 | 36 | 61 | 3 | |
| 70-90 | Calcic | **calc.**, felds., smec. | 7.87 | 82.75 | 1.6 | <0.1 | 15 | 65 | 20 | |
| **B150** | | | | | | | | | | $8*10^{-7}$ |
| 0-10 | Mollic | **felds.**, smec. | 7.29 | 80.16 | 0.2 | 3.9 | 55 | 45 | 0 | |
| 10-40 | Cambic | **felds.**, smec. | NA | NA | 0.3 | NA | 50 | 50 | 0 | |
| 40-50 | Vertic | **felds.**, smec. | 7.60 | 78.87 | 0.1 | 0.9 | 52 | 48 | 0 | |
| 50-70 | Vertic | **felds.**, smec. | NA | NA | 0.1 | NA | 55 | 45 | 0 | |
| 70-90 | Vertic | **felds.**, smec. | 7.82 | 69.97 | 0.2 | 1.3 | 54 | 46 | 0 | |
| 90-100 | Vertic | **felds.**, smec. | 7.76 | 72.25 | 0.6 | 0.0 | 55 | 45 | 0 | |
| **C60** | | | | | | | | | | $1*10^{-5}$ |
| 0-10 | Mollic, calcic | **qtz.,** calc., felds. | 7.24 | 80.36 | 0.5 | 4.9 | 63 | 37 | 0 | |
| 10-30 | Calcic | **qtz.,** calc., felds. | 7.67 | 77.87 | 0.6 | 1.3 | 32 | 64 | 4 | |
| 30-50 | Cambic | **qtz.,** calc., felds. | 7.62 | 84.55 | 0.8 | 0.9 | 31 | 69 | 0 | |
| 50-70 | Cambic | **calc.,** qtz., felds. | 7.79 | 79.61 | 1.9 | <0.1 | 40 | 60 | 0 | |
| **C155** | | | | | | | | | | $3*10^{-5}$ |
| 0-10 | Mollic, | **calc.**, felds., smec. | 7.32 | 83.01 | 1.4 | 2.0 | 32 | 63 | 5 | |
| 10-50 | Cambic | **calc.**, felds., smec. | 7.59 | 79.49 | 1.5 | 0.9 | 31 | 61 | 8 | |
| 50-70 | Calcic | **calc.**, felds., smec. | 7.84 | 80.99 | 2.1 | 0.2 | 33 | 56 | 11 | |
| 70-100 | calcic | **calc.**, felds., smec. | 7.91 | 82.63 | 1.9 | <0.1 | 10 | 82 | 8 | |
| **C220** | | | | | | | | | | $7*10^{-5}$ |
| 0-10 | Mollic, calcic | **calc.**, felds., smec. | 7.24 | 65.97 | 3.7 | 4.9 | 24 | 65 | 11 | |
| 20-50 | Calcic | **calc.**, felds., smec. | 7.90 | 55.12 | 4.9 | 0.5 | 28 | 52 | 20 | |
| 50-60 | Calcic | **calc.**, felds., smec. | 8.14 | 50.80 | 5.6 | 0.2 | NA | NA | NA | |

**Table 2 –** Elemental contents (expressed in g $kg^{-1}$ or mg $kg^{-1}$) and Sr isotope ratios in soil and rock samples. P-values of one-sided Mann Whitney U-test (MWU-test) between all horizons of the two catenas were performed to evidence significant differences. Differences are considered significant if $p \leq 0.05$ and are annotated with a*.

| | Type | Depth | Mg | Al | P | K | Ca | Mn | Fe | S | Cu | Zn | Sr | Mo | Ba | $^{87}Sr/^{86}Sr$ | 2SD |
|---|---|---|---|---|---|---|---|---|---|---|---|---|---|---|---|---|---|
| | | | g $kg^{-1}$ | g $kg^{-1}$ | g $kg^{-1}$ | g $kg^{-1}$ | g $kg^{-1}$ | g $kg^{-1}$ | g $kg^{-1}$ | mg $kg^{-1}$ | mg $kg^{-1}$ | mg $kg^{-1}$ | mg $kg^{-1}$ | mg $kg^{-1}$ | mg $kg^{-1}$ | | |
| B20 | Bulksoil | 0-10 | 19.36 | 56.28 | 2.85 | 7.10 | 86.35 | 1.00 | 62.08 | 679 | 356.6 | 162 | 257 | 1.02 | 282 | 0.7056 | 0.00011 |
| B20 | Bulksoil | 10-50 | 20.37 | 56.12 | 2.24 | 5.90 | 107.34 | 1.02 | 66.83 | 317 | 209.6 | 138 | 295 | 1.03 | 299 | - | - |
| B20 | Bulksoil | 50-70 | 12.52 | 36.96 | 1.75 | 4.05 | 40.82 | 1.08 | 75.40 | - | 91.0 | 125 | 256 | 0.94 | 257 | 0.7047 | 0.0001 |
| B20 | Bulksoil | 110-120 | 10.90 | 57.53 | 1.03 | 4.23 | 23.34 | 1.35 | 84.36 | 76 | 63.6 | 118 | 179 | 0.57 | 258 | 0.7051 | 0.00008 |
| B60 | Bulksoil | 0-10 | 15.83 | 49.21 | 3.36 | 7.17 | 42.37 | 1.18 | 66.74 | 965 | 563.7 | 196 | 221 | 1.36 | 306 | 0.7054 | 0.00011 |
| B60 | Bulksoil | 10-30 | 17.71 | 61.77 | 1.78 | 4.12 | 39.62 | 1.16 | 72.27 | - | 135.9 | 115 | 193 | 1.06 | 265 | - | - |
| B60 | Bulksoil | 30-60 | 11.70 | 54.29 | 1.57 | 4.45 | 32.68 | 1.33 | 77.28 | 177 | 79.9 | 112 | 188 | 0.90 | 301 | 0.7057 | 0.00013 |
| B60 | Bulksoil | 60-70 | 15.55 | 51.80 | 1.79 | 6.25 | 31.78 | 1.15 | 82.37 | - | 56.7 | 112 | 176 | 2.69 | 342 | - | - |
| B60 | Bulksoil | 70-90 | 33.04 | 50.89 | 4.17 | 2.39 | 95.64 | 0.97 | 77.08 | - | 40.3 | 101 | 406 | 1.17 | 373 | 0.7053 | 0.00013 |
| B150 | Bulksoil | 0-10 | 7.93 | 36.57 | 3.34 | 8.76 | 31.16 | 1.08 | 71.77 | 547 | 277.0 | 163 | 250 | 1.40 | 343 | 0.7043 | 0.00011 |
| B150 | Bulksoil | 40-50 | 8.62 | 46.07 | 2.42 | 6.09 | 27.82 | 1.27 | 83.35 | 155 | 72.8 | 140 | 217 | 1.25 | 296 | 0.7043 | 0.00011 |
| B150 | Bulksoil | 70-90 | 18.22 | 61.35 | 2.88 | 7.48 | 45.06 | 1.20 | 93.37 | - | 61.0 | 139 | 420 | 1.34 | 394 | - | - |
| B150 | Bulksoil | 90-100 | 17.95 | 70.39 | 3.05 | 7.92 | 52.64 | 1.32 | 98.88 | - | 59.1 | 133 | 441 | 1.46 | 424 | 0.7037 | 0.00009 |

| | | | | | | | | | | | | | | | | |
|---|---|---|---|---|---|---|---|---|---|---|---|---|---|---|---|---|
| C60 | Bulksoil | 0-10 | 9.94 | 47.98 | 3.29 | 9.02 | 35.16 | 1.13 | 72.18 | 707 | 351.9 | 177 | 137 | 0.91 | 394 | 0.7067 | 0.00009 |
| C60 | Bulksoil | 10-30 | 5.39 | 39.17 | 2.64 | 6.82 | 32.46 | 0.95 | 60.33 | 255 | 186.5 | 131 | 128 | 0.70 | 344 | 0.7066 | 0.00011 |
| C60 | Bulksoil | 30-50 | 14.54 | 56.04 | 2.44 | 6.11 | 44.11 | 1.08 | 71.93 | - | 160.5 | 134 | 152 | 0.82 | 413 | - | - |
| C60 | Bulksoil | 50-70 | 23.01 | 55.10 | 3.25 | 4.65 | 92.3 | 1.07 | 74.01 | - | 83.9 | 119 | 178 | 0.60 | 386 | 0.7064 | 0.00008 |
| C155 | Bulksoil | 0-10 | 23.08 | 57.24 | 3.55 | 6.92 | 71.22 | 0.96 | 70.68 | 400 | 164.7 | 132 | 152 | 0.68 | 497 | 0.7061 | 0.00011 |
| C155 | Bulksoil | 10-50 | 22.7 | 53.08 | 2.92 | 4.61 | 73.03 | 0.92 | 68.88 | 254 | 124.9 | 119 | 153 | 0.69 | 475 | 0.7061 | 0.00009 |
| C155 | Bulksoil | 50-70 | 23.25 | 52.57 | 3.03 | 4.05 | 89.64 | 0.99 | 73.49 | - | 111.2 | 123 | 171 | 0.70 | 504 | - | - |
| C155 | Bulksoil | 70-100 | 27.50 | 60.79 | 3.57 | 2.77 | 92.84 | 0.92 | 73.07 | - | 37.3 | 113 | 147 | 0.48 | 563 | - | - |
| C220 | Bulksoil | 0-10 | 12.87 | 33.72 | 3.17 | 5.21 | 135.1 | 0.70 | 42.68 | 784 | 261.9 | 157 | 187 | 0.90 | 286 | 0.7069 | 0.0001 |
| C220 | Bulksoil | 20-50 | 14.23 | 40.23 | 2.24 | 2.80 | 194.42 | 0.66 | 46.29 | 240 | 69.8 | 83 | 217 | 0.98 | 300 | 0.7068 | 0.0001 |
| C220 | Bulksoil | 50-60 | 11.31 | 36.49 | 1.98 | 1.37 | 232.26 | 0.42 | 35.76 | 168 | 31.4 | 66 | 196 | 0.69 | 137 | 0.7071 | 0.0001 |
| MWU-test | p-value | | 0.32 | 0.14 | 0.08 | 0.17 | 0.02* | <0.01* | 0.01* | 0.40 | 0.41 | 0.24 | <0.01* | <0.01* | 0.02* | <0.01* | |
| Basalt | Rock | | 44.22 | 55.91 | 2.96 | 9.87 | 55.34 | 1.25 | 81.86 | - | 49.1 | 120 | 1516 | 1.10 | 930 | 0.7032 | 0.00001 |
| Tufa | Rock | | 17.28 | 46.15 | 2.72 | 2.16 | 105.42 | 0.83 | 52.95 | - | 44.0 | 68 | 173 | 0.17 | 903 | 0.7067 | 0.00009 |
| Limestone | Rock | | 3.07 | 0.86 | 0.33 | 0.10 | 394.17 | 0.67 | 3.32 | - | 2.6 | 4 | 169 | 0.25 | 10 | 0.707 | 0.00002 |

***NB: Cu isotope ratios are presented in Blotevogel et al. (2018)***

**Table 3 –** Elemental contents (expressed in g $kg^{-1}$ or mg $kg^{-1}$) in leaves and grapes, and C, Sr and Cu isotope ratios in leaves. P-values of one-sided Mann Whitney U-test (MWU-test) between the two catenas were performed to evidence significant differences between the two plots. Differences are considered significant if $p \leq 0.05$ and are annotated with a*.

| Sample | Type | N | Mg | P | S | K | Ca | Al | Mn | Fe | Cu | Zn | Sr | Mo | Ba | K/Ca | $\delta^{13}C$ | 2SD | 87Sr/86Sr | 2SD | $\delta^{65}Cu$ | 2SD |
|---|---|---|---|---|---|---|---|---|---|---|---|---|---|---|---|---|---|---|---|---|---|---|
| | | g $kg^{-1}$ | g $kg^{-1}$ | g $kg^{-1}$ | g $kg^{-1}$ | g $kg^{-1}$ | g $kg^{-1}$ | mg $kg^{-1}$ | mg $kg^{-1}$ | mg $kg^{-1}$ | mg $kg^{-1}$ | mg $kg^{-1}$ | mg $kg^{-1}$ | mg $kg^{-1}$ | mg $kg^{-1}$ | mol $mol^{-1}$ | ‰ | ‰ | | | ‰ | ‰ |
| B20 | Leaf | 13.04 | 2.81 | 2.24 | 1.63 | 6.85 | 29.7 | 24.4 | 35.7 | 33 | 99.3 | 18.4 | 49.9 | 0.118 | 8.79 | 0.24 | -26.56 | 0.22 | 0.7065 | 0.00008 | -1.735 | 0.098 |
| B60 | Leaf | 12.77 | 2.95 | 2.53 | 1.41 | 7.05 | 31.7 | 25.3 | 23 | 34.4 | 70.5 | 24.1 | 66.3 | 0.036 | 8.34 | 0.23 | -27.64 | 0.12 | 0.7061 | 0.00012 | -1.28 | 0.1 |
| B150 | Leaf | 15.14 | 4.24 | 2.39 | 1.44 | 4.67 | 32.1 | 27.1 | 51.9 | 44.3 | 43.6 | 23.2 | 54.2 | 0.042 | 18.41 | 0.15 | -26.30 | 0.24 | 0.7062 | 0.00001 | -1.067 | 0.1 |
| C60 | Leaf | 14.03 | 3.15 | 2.14 | 1.78 | 8.4 | 26.9 | 29.9 | 49.6 | 64.2 | 125.4 | 25.6 | 43.1 | 0.271 | 36.14 | 0.32 | -26.54 | 0.33 | 0.7072 | 0.00009 | -1.833 | 0.055 |
| C155 | Leaf | 15.00 | 5.49 | 4.08 | 1.67 | 7.32 | 37.7 | 25.3 | 58.8 | 40.6 | 33.9 | 35.2 | 48.7 | 0.166 | 22.65 | 0.20 | -26.96 | 0.05 | 0.7068 | 0.00012 | -0.863 | 0.102 |
| C220 | Leaf | 15.80 | 2.74 | 2.77 | 1.6 | 9.04 | 32.6 | 40.7 | 47.9 | 45.7 | 74.3 | 28.8 | 38.6 | 0.114 | 20.42 | 0.29 | -27.02 | 0.05 | 0.707 | 0.00013 | -1.134 | 0.009 |
| MWU-test | p-value | 0.20 | 0.50 | 0.35 | 0.10 | 0.05* | 0.35 | 0.13 | 0.20 | 0.10 | 0.50 | 0.05* | 0.05* | 0.10 | 0.05* | 0.20 | 0.50 | | 0.05* | | 0.50 | |
| B20 | Grape | 3.33 | 0.72 | 1.37 | | 9.21 | 2.37 | 4.80 | 2.90 | 8.11 | 5.83 | 5.05 | 5.38 | 0.028 | 1.15 | 3.99 | -24.5 | 0.83 | | | | |

| | | | | | | | | | | | | | | | | | |
|---|---|---|---|---|---|---|---|---|---|---|---|---|---|---|---|---|---|
| B60 | Grape | 1.00 | 0.52 | 1.25 | 10.40 | 1.69 | 4.55 | 1.87 | 8.95 | 5.73 | 3.15 | 3.18 | 0.027 | 0.50 | 6.33 | -24.65 | 0.19 |
| B150 | Grape | 3.38 | 0.70 | 1.25 | 8.41 | 2.08 | 5.03 | 6.04 | 10.87 | 4.92 | 4.11 | 3.47 | 0.030 | 1.28 | 4.16 | -24.27 | 0.52 |
| C60 | Grape | 2.28 | 0.54 | 1.31 | 10.53 | 1.46 | 5.05 | 4.40 | 9.64 | 6.88 | 3.97 | 2.43 | 0.046 | 2.17 | 7.41 | -24.29 | 0.58 |
| C155 | Grape | 2.51 | 0.56 | 1.44 | 10.83 | 1.45 | 5.10 | 2.62 | 9.40 | 4.82 | 4.12 | 1.57 | 0.049 | 0.90 | 7.68 | -25.82 | 0.48 |
| C220 | Grape | 2.81 | 0.51 | 1.33 | 11.16 | 1.45 | 7.08 | 2.94 | 10.07 | 5.79 | 3.19 | 1.93 | 0.053 | 1.01 | 7.91 | -24.56 | 0.01 |
| MWU-test | | 0.35 | 0.20 | 0.19 | 0.05 | 0.04* | 0.05* | 0.50 | 0.35 | 0.50 | 0.50 | 0.05* | 0.05* | 0.50 | 0.05* | 0.35 | |